Site-specific ubiquitination exposes a linear motif to promote interferon-α receptor endocytosis

K.G. Suresh Kumar,[1,2] Hervé Barriere,[3,4] Christopher J. Carbone,[1,2] Jianghuai Liu,[1,2] Gayathri Swaminathan,[1,2] Ping Xu,[5] Ying Li,[1,2] Darren P. Baker,[6] Junmin Peng,[5] Gergely L. Lukacs,[3,4] and Serge Y. Fuchs[1,2]

[1]Department of Animal Biology and [2]Mari Lowe Center for Comparative Oncology Research, School of Veterinary Medicine, University of Pennsylvania, Philadelphia, PA 19104
[3]Program in Cell and Lung Biology, Hospital for Sick Children Research Institute, Department of Laboratory Medicine and Pathobiology and [4]Department of Biochemistry, University of Toronto, Toronto, Ontario M5G 1X8, Canada
[5]Department of Human Genetics, Center for Neurodegenerative Disease, Emory University, Atlanta, GA 30322
[6]Biogen Idec, Inc., Cambridge, MA 02142

Ligand-induced endocytosis and lysosomal degradation of cognate receptors regulate the extent of cell signaling. Along with linear endocytic motifs that recruit the adaptin protein complex 2 (AP2)–clathrin molecules, monoubiquitination of receptors has emerged as a major endocytic signal. By investigating ubiquitin-dependent lysosomal degradation of the interferon (IFN)-α/β receptor 1 (IFNAR1) subunit of the type I IFN receptor, we reveal that IFNAR1 is polyubiquitinated via both Lys48- and Lys63-linked chains. The SCF$^{\beta Trcp}$ (Skp1–Cullin1–F-box complex) E3 ubiquitin ligase that mediates IFNAR1 ubiquitination and degradation in cells can conjugate both types of chains in vitro. Although either polyubiquitin linkage suffices for postinternalization sorting, both types of chains are necessary but not sufficient for robust IFNAR1 turnover and internalization. These processes also depend on the proximity of ubiquitin-acceptor lysines to a linear endocytic motif and on its integrity. Furthermore, ubiquitination of IFNAR1 promotes its interaction with the AP2 adaptin complex that is required for the robust internalization of IFNAR1, implicating cooperation between site-specific ubiquitination and the linear endocytic motif in regulating this process.

Introduction

The extent of ligand-induced cell signaling is negatively regulated by cognate receptor endocytosis that is mediated by both clathrin-dependent and independent pathways. Cargo-specific clathrin-dependent endocytosis occurs via an interaction of clathrin lattices formed on the plasma membrane with cargo receptors and relies on adaptor complexes (e.g., adaptin protein complex 2 [AP2] and Dab), which recognize specific linear endocytic motifs present within the cytoplasmic domains of the target receptor. For example, the AP50/μ2 subunit of AP2 recognizes Tyr-based motifs and enables AP2-dependent tethering of cargo to clathrin molecules (Smythe and Warren, 1991; for review see Bonifacino and Traub, 2003).

In addition to the linear endocytic motifs, ubiquitin has emerged as an important internalization signal for numerous eukaryotic plasma membrane proteins (Bonifacino and Weissman, 1998; Hicke and Dunn, 2003). However, the nature of ubiquitination and the topology of the polyubiquitin chain as well as their requirement for internalization and/or postinternalization sorting vary widely among different cargo substrates and remain poorly understood. For example, monoubiquitination is required for the internalization of many yeast receptors but not of mammalian EGF receptor (EGFR). However, ubiquitination is essential for directing EGFR to the lysosome (Levkowitz et al., 1998; Huang et al., 2006). Furthermore, although EGFR undergoes polyubiquitination predominantly via K63-linked chains (Huang et al., 2006), multiple monoubiquitination of EGFR is sufficient for promoting its endocytosis (Haglund et al., 2003a; Mosesson et al., 2003).

The current paradigm (supported by studies on chimerical receptor-ubiquitin fusion proteins in yeast and mammalian cells) suggests that monoubiquitination promotes the internalization and sorting of cargo receptors by recruiting ubiquitin-binding proteins, which link cargo to the components of endocytic and sorting machinery (Dikic, 2003; Haglund et al., 2003a; Hicke and Dunn, 2003; Polo et al., 2003; Raiborg et al., 2003; Sigismund et al., 2004). Interpretation of this model would predict that neither

K.G.S. Kumar and H. Barriere contributed equally to this paper.

Correspondence to Serge Y. Fuchs: syfuchs@vet.upenn.edu

Abbreviations used in this paper: AP, adaptin protein complex; βTrcp, β-transducin repeats–containing protein; EGFR, EGF receptor; FRIA, fluorescence ratio image analysis; HBS, Hepes-buffered saline; IFNAR1, IFN-α/β receptor 1; MESNA, 2-mercaptoethanesulfonic acid; SCF, Skp1–Cullin1–F-box complex; shRNA, short hairpin RNA.

The online version of this article contains supplemental material.

The Journal of Cell Biology, Vol. 179, No. 5, December 3, 2007 935–950
http://www.jcb.org/cgi/doi/10.1083/jcb.200706034

the topology of ubiquitin chains nor the site of ubiquitin conjugation should determine the efficiency of endocytosis.

However, in addition to monoubiquitin, K63-linked polyubiquitin chains are required for endocytosis of yeast uracil permease (Galan and Haguenauer-Tsapis, 1997; Blondel et al., 2004; Dupre et al., 2004). This linkage also regulates endocytosis of several mammalian proteins, including nerve growth factor receptor TrkA (Geetha et al., 2005), major histocompatibility complex class I and II proteins (Duncan et al., 2006; Ohmura-Hoshino et al., 2006; Shin et al., 2006; van Niel et al., 2006), aquaporin-2 water channel (Kamsteeg et al., 2006), and some chimerical ubiquitin fusion model proteins (Barriere et al., 2006; Hawryluk et al., 2006). Intriguingly, the lysosomal degradation of Deltex, a regulator of the Notch pathway, might require K29-linked chains (Chastagner et al., 2006).

It is plausible that the polyubiquitination of receptors provides an advantage over monoubiquitination by increasing the number of interacting modules and, thus, the affinity of interaction between ubiquitinated cargos and ubiquitin-binding proteins (Hawryluk et al., 2006; Traub and Lukacs, 2007). Nevertheless, such increased interactions alone can hardly provide an explanation for how the use of various types of ubiquitination and of diverse ubiquitin chains might contribute to different stages of the endocytosis of various cargo receptors. One potential explanation for such diversity is that the unique linear determinants within the cytoplasmic tails of individual receptors may play a role in ubiquitin-mediated events to ensure the most efficient internalization and/or sorting.

We have investigated the mechanisms that regulate the turnover of INF-α/β receptor 1 (IFNAR1), a chain of type I IFN receptor that plays a key role in antiviral defense (Constantinescu et al., 1994; Muller et al., 1994). Lysosomal degradation of IFNAR1 requires its ubiquitination (mainly on a cluster of lysine residues, including K501, K525, and K526) by the $SCF^{\beta Trcp}$ (Skp1–Cullin1–F-box complex) E3 ubiquitin ligase. This E3 ligase binds to the $_{534}$DSGNYS phosphodegron within the cytoplasmic tail of IFNAR1; phosphorylation of S535 and S539 residues within this degron is stimulated by the ligand treatment (Kumar et al., 2003, 2004). In this study, we investigated the role of ubiquitination in internalization, postinternalization sorting, and lysosomal degradation of IFNAR1. We report that although polyubiquitination is sufficient for postinternalization sorting of IFNAR1, the maximal rate of IFNAR1 internalization and degradation requires not only both K48 and K63 linkages but also site-specific ubiquitination and its interaction with a linear endocytic motif within the cytoplasmic tail of IFNAR1.

Results

Both K48- and K63-linked polyubiquitin chains are present on IFNAR1 and can be formed by $SCF^{\beta Trcp}$

The intracellular domain of IFNAR1 contains six Lys residues, three of which (K501, K525, and K526) form a cluster that is critical for efficient ubiquitination and degradation given that substitution of these three Lys to Arg results in a ubiquitination-deficient and stable mutant, termed $IFNAR1^{KR}$ (Kumar et al., 2004). Coexpression of IFNAR1 with HA-tagged ubiquitin followed by denaturing immunoprecipitation of IFNAR1 revealed an HA-reactive smear (Fig. 1 A) whose apparent molecular mass is greater than expected from IFNAR1 that undergoes multiple monoubiquitination (110 kD + (8 kD × 6) = 158 kD), suggesting that IFNAR1 might be polyubiquitinated. Indeed, direct determination of the ubiquitinated species of IFNAR1 purified from cells using a quantitative mass spectrometry approach revealed the presence of polyubiquitin chains (that included both K48 and K63 linkages but not other types of chains) on both $IFNAR1^{WT}$ and $IFNAR1^{KR}$, in which the latter protein expectedly exhibited less overall levels of ubiquitin linkages (Fig. 1 B and Fig. S1, available at http://www.jcb.org/cgi/content/full/jcb.200706034/DC1; and not depicted).

The presence of the K63-linked ubiquitin chains on IFNAR1 was surprising given that (1) the $SCF^{\beta Trcp}$ E3 ubiquitin ligase is a major regulator of IFNAR1 ubiquitination (Kumar et al., 2003) and (2) this ubiquitin ligase generally targets its substrates for proteasomal degradation (Harper et al., 2002; Fuchs et al., 2004; Petroski and Deshaies, 2005), which preferentially utilizes the K48-linked chains (Pickart and Fushman, 2004). Therefore, we determined the ability of $SCF^{\beta Trcp}$ to catalyze the ligation of polyubiquitin chains using ubiquitin mutants that lack all Lys residues except either Lys48 (R48K) or Lys63 (R63K). In the presence of either UbcH5c or Cdc34 (as an E2 ubiquitin–conjugating enzyme), purified $SCF^{\beta Trcp}$ indeed facilitated the formation of both types of chains (Fig. 1 C), indicating that linkages of both types could be formed by this E3 ubiquitin ligase in vitro.

Both K48- and K63-linked polyubiquitin chains are required for efficient IFNAR1 degradation

We next sought to investigate the role of polyubiquitination and different ubiquitin chain topologies in the degradation of IFNAR1. Currently, the only approach available to address this question in mammalian cells is the forced expression of various ubiquitin mutants to overcome the functions of endogenous ubiquitin. This approach is a standard methodology for delineating the role of diverse ubiquitin chains in receptor internalization and turnover (Haglund et al., 2003b; Mosesson et al., 2003; Duncan et al., 2006). We have used this approach together with an IFNAR1 degradation assay (measured by IFNAR1 levels in cells treated with protein synthesis inhibitor cycloheximide; further termed cycloheximide chase), in which treatment with the ligand robustly increases IFNAR1 turnover (Fig. 2 A).

Expression of a lysine-less ubiquitin mutant (K0) interfered with the formation of high molecular weight bands that react with antiubiquitin antibody and represent polyubiquitinated proteins (Fig. S1 B). Cells transfected with K0 exhibited a delayed degradation of either endogenous or cotransfected IFNAR1 in comparison with cells expressing wild-type ubiquitin (Fig. 2, B and C) or empty vector (Fig. S1 C). Expression of K0 mutant also decreased the efficiency of the ubiquitination of endogenous (Fig. 2 D) or exogenously expressed (not depicted) IFNAR1 in cells. Although these results are consistent with idea that polyubiquitination of IFNAR1 is required for its turnover,

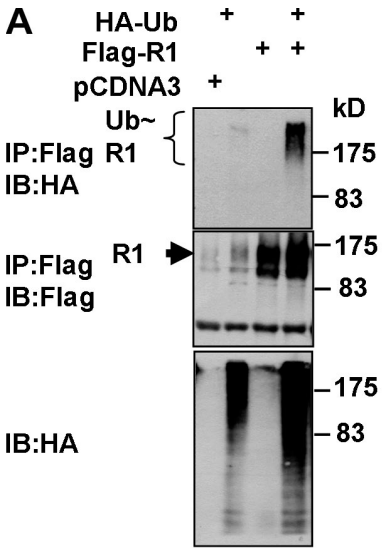

B

	Ub links total, pmoles	Links type, % K48	K63
Vector	0.003	0.0	100
IFNAR1 WT	0.165± 0.009	57.1	42.9
IFNAR1 KR	0.032± 0.005	68.8	31.2

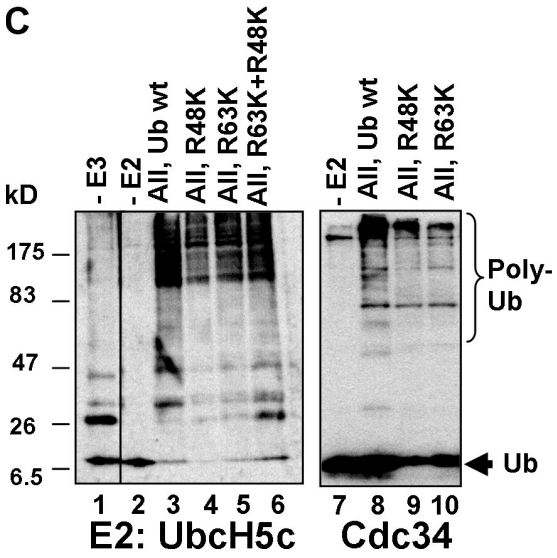

Figure 1. **Both K48- and K63-linked polyubiquitin chains are present on IFNAR1 in cells and can be formed by SCF$^{\beta Trcp}$ in vitro.** (A) In vivo ubiquitination of IFNAR1 expressed in 293T cells as indicated, purified via denaturing immunoprecipitation and analyzed by immunoblotting using the indicated antibodies. (B) Amount of IFNAR1-conjugated polyubiquitin chain links (in pmoles) and relative percentage of K48 and K63 linkages found in these preparations were measured by the absolute quantification of ubiquitin adducts technique. (C) In vitro formation of polyubiquitin chains by the SCF$^{\beta Trcp}$ E3 ligase. Recombinant SCF$^{\beta Trcp}$ (absent in lane 1) was incubated with E1, E2 (UbcH5c or Cdc34 as indicated), biotinylated ubiquitin (wt, lanes 1–3 and 7–8; R48K, lanes 4, 6, and 9; R63K, lanes 5, 6, and 10), and ATP. The reaction was analyzed by immunoblotting using HRP-conjugated streptavidin.

the expression of K0 might interfere with upstream events essential for IFNAR1 ubiquitination such as IFNAR1 phosphorylation within the phosphodegron or with β-transducin repeats–containing protein (βTrcp) recruitment. However, the expression of K0 did not inhibit IFNAR1 phosphorylation on Ser535. To the contrary, this ubiquitin mutant's expression resulted in the accumulation of phosphorylated IFNAR1 in untreated cells, further indicating the role of polyubiquitination in the degradation of IFNAR1 (Fig. 2 E). Furthermore, the K0 mutant did not inhibit the recruitment of βTrcp to either IFNAR1 (Fig. 2 F) or to other SCF components (Fig. 2 G). Together, these results indicate that IFNAR1 is polyubiquitinated and that K0 might directly inhibit IFNAR1 polyubiquitination (and polyubiquitination-dependent turnover) by capping (i.e., interfering with the elongation of polyubiquitin chains on IFNAR1).

We next tested whether interfering with a specific type of polyubiquitin chain would affect the proteolysis of IFNAR1 (measured by a cycloheximide chase assay) using the expression of various point or reverse ubiquitin mutants (Fig. S1 B). Although the expression of K48R but not of K63R ubiquitin mutant stabilized a proteasomal substrate c-Jun, either of these ubiquitin mutants decreased the rate of degradation of both endogenous (Fig. 3 A) and exogenously expressed (Fig. 3 B) IFNAR1. Consistent with more abundant K48 linkages found on Flag-tagged IFNAR1 (Fig. 1 B), K48R mutant was more efficient in stabilizing exogenous IFNAR1 than K63R mutant, indicating that a fraction of exogenous IFNAR1 might undergo intracellular K48-dependent proteasomal degradation that may occur in the biosynthetic pathway. Given that K29R mutant did not affect IFNAR1 turnover (Fig. 3 B) while being expressed at similar levels as K48R and K63R (Fig. S1 B), it is likely that both K48- and K63-linked (but not K29 linked) ubiquitin chains are important for the efficient degradation of IFNAR1. Remarkably, the expression of neither of these ubiquitin point mutants substantially affected the overall extent of IFNAR1 ubiquitination that was noticeably inhibited by K0 (Fig. 3 C) despite its relatively low level of expression (Fig. S1 B). These data suggest that formation of indiscriminate types of polyubiquitin chains may not suffice for efficient IFNAR1 degradation under conditions in which either K48 or K63 linkage is inhibited.

To corroborate these conclusions, we tested the effects of expression of the reverse ubiquitin mutants, in which all lysine residues except either K48 (R48K) or K63 (R63K) were mutated to arginines. When expressed separately, these mutants inhibited IFNAR1 degradation similarly to an effect of K0 (and to a lesser extent than that produced by point K48R or K63R mutants, most likely as a result of the difference in expression levels; Fig. S1 B). However, coexpression of both R48K and R63K mutants together alleviated a delay in IFNAR1 degradation (when compared with the effects of K0 or either of these reverse mutants alone; Fig. 3 D). This combination of R48K and R63K also yielded a noticeably higher overall extent of IFNAR1 ubiquitination (compared with either of these mutants alone; Fig. 3 E). These data, together with mass spectrometry results, support a model wherein the polyubiquitination of IFNAR1 is necessary but not sufficient for its robust degradation.

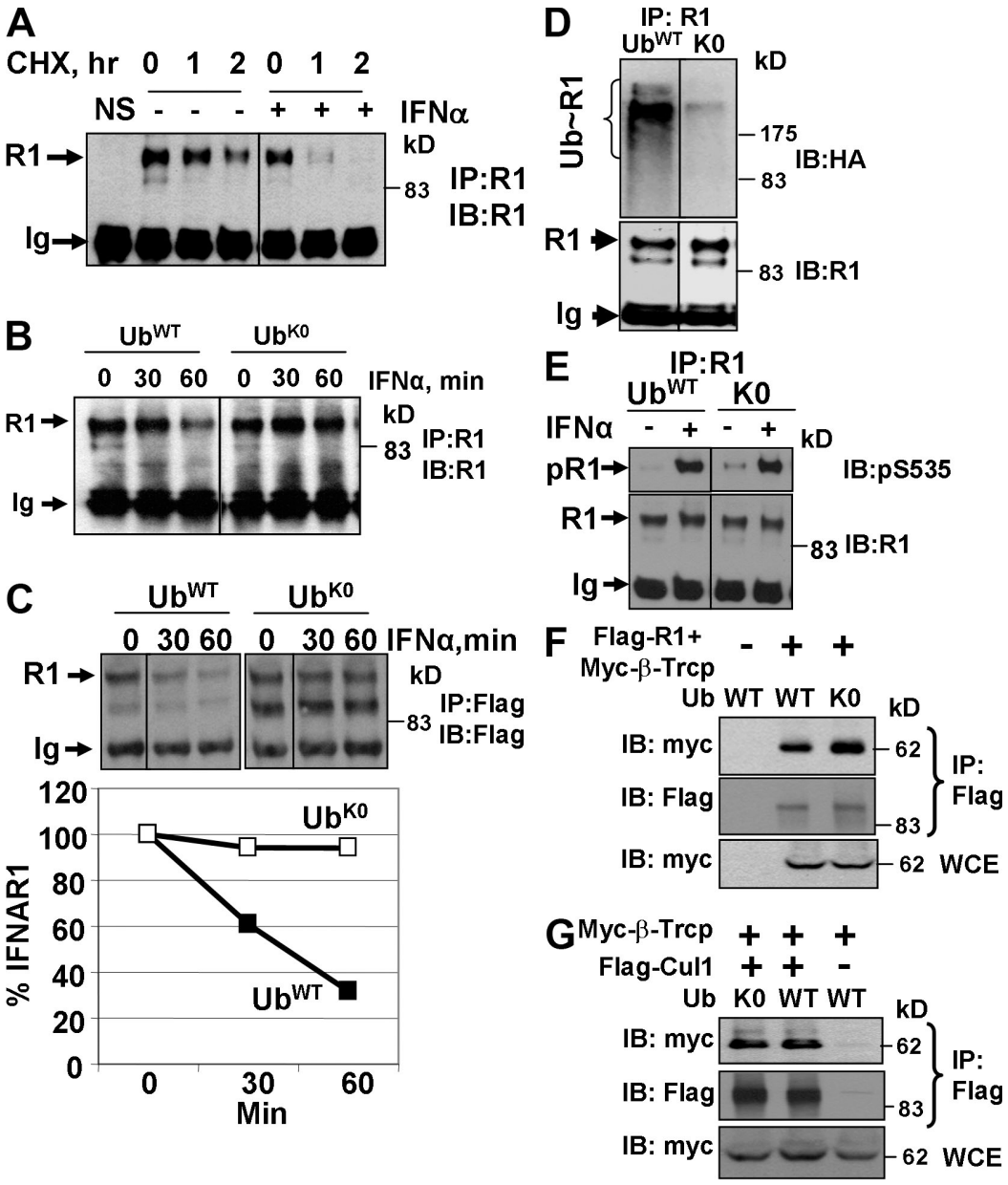

Figure 2. **Polyubiquitination is required for IFNAR1 degradation but is dispensable for the phosphorylation of IFNAR1 and its interaction with βTrcp as well as for assembly of the SCF$^{\beta Trcp}$ E3 ubiquitin ligase.** (A) Treatment of cells with IFN stimulates the degradation of endogenous IFNAR1, which was measured as IFNAR1 levels in lysates from cells treated by cycloheximide (a cycloheximide chase) detected by immunoprecipitation/immunoblotting using anti-IFNAR1 antibodies. Control precipitation (NS) was performed using an isotype monoclonal antibody. Positions of fully glycosylated mature IFNAR1 (Ragimbeau et al., 2003) and heavy chain of Igs are indicated by the arrows. (B) Degradation of endogenous IFNAR1 in the presence of IFN-α was analyzed by cycloheximide chase in as in A. (C) Degradation of exogenous IFNAR1 in cells coexpressed with either wild-type ubiquitin or K0 mutant analyzed by cycloheximide chase in the presence of IFN-α using anti-Flag antibody. Results are graphed as a percentage of IFNAR1 remaining at the indicated time points of a chase. (D) Ubiquitination of endogenous IFNAR1 in the IFN-α–treated cells expressing either wild-type or K0 ubiquitin mutant was assessed as in Fig. 1 A. (E) Ser535 phosphorylation of endogenous IFNAR1 in cells expressing either wild-type or K0 ubiquitin mutant and treated or not treated with IFN-α was assessed by immunoprecipitation followed by immunoblotting using the indicated antibodies. (F and G) Effects of K0 expression on the recruitment of myc-tagged βTrcp to either Flag-tagged IFNAR1 (F) or Flag-tagged Cullin1 (G) were analyzed by coimmunoprecipitation followed by immunoblotting using the indicated antibodies. WCE, whole cell extract.

Nonspecific polyubiquitination is necessary and sufficient for postinternalization sorting of IFNAR1 toward lysosomes

Given that ubiquitination is essential for postinternalization sorting of many signaling receptors, including EGFR (Levkowitz et al., 1998; Huang et al., 2006), we tested whether IFNAR1 sorting also requires ubiquitination. Immunocytochemical analysis showed that internalized wild-type IFNAR1 mostly colocalized with fluorophor-conjugated dextran (which is targeted to the late endosomes/lysosomes; Fig. S2, available at http://www.jcb.org/cgi/content/full/jcb.200706034/DC1) but not with transferrin (that is localized in early/recycling endosomes). However, an opposite pattern was seen for the partially ubiquitination-deficient IFNAR1^{KR} mutant, who colocalized predominantly

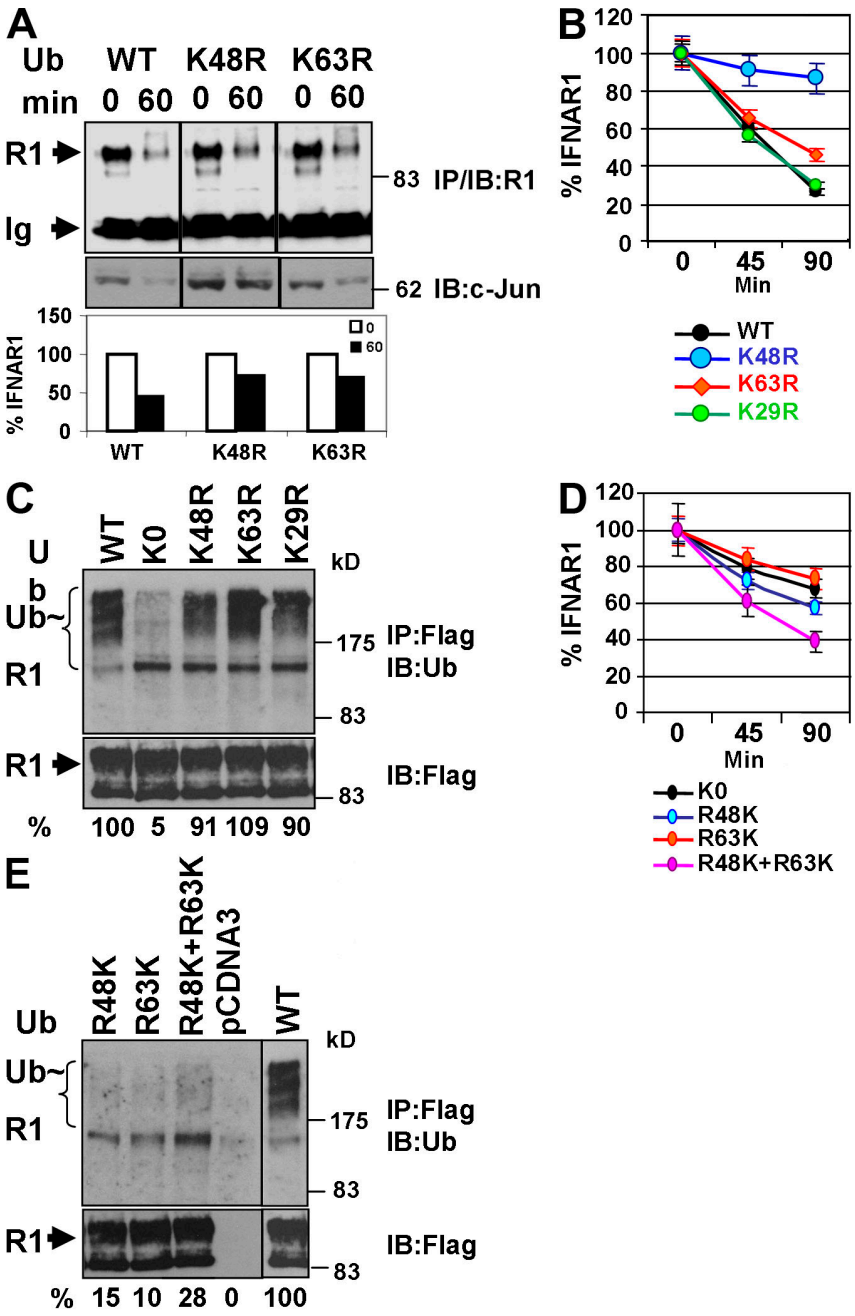

Figure 3. **Role of specific polyubiquitin chains in IFNAR1 ubiquitination and degradation.** (A, B, and D) Effect of expression of various ubiquitin mutants on the degradation of endogenous (A) and exogenous (B and D) IFNAR1 was assessed via cycloheximide chase in the presence of IFN-α as in Fig. 2 C. Data are represented as the average ± SEM (error bars). (C and E) Effect of these ubiquitin mutants' expression on the extent of IFNAR1 ubiquitination was measured similarly to the experiment shown in Fig. 1 A using antiubiquitin antibody. Ratios between ubiquitin and IFNAR1 signals were calculated as the percentage of such for wild-type ubiquitin (assigned a value of 100%).

with transferrin and not with dextran (Fig. 4 A). This result suggests that ubiquitination might be required for efficient sorting of IFNAR1 into the lysosomes.

To verify this conclusion quantitatively, we used fluorescence ratio image analysis (FRIA; see Materials and methods; Sharma et al., 2004) that determines the sorting efficiency of internalized receptors from early endosomes to the lysosomal compartment. This analysis is based on monitoring the luminal pH of cargo-containing vesicles (pH_v) and relies on the distinct pH_v of early/recycling endosomes (pH of ~6.4–6.5) and late endosomes/lysosomes (pH < 5.5; Mukherjee et al., 1997). Additional control experiments verified that the antibody used did not dissociate from the receptor in a moderately acidic environment (pH of ~5.0; Fig. S3 A, available at http://www.jcb.org/cgi/content/full/jcb.200706034/DC1), thus allowing these measurements.

Although a mean pH_v of internalized wild-type IFNAR1-containing vesicles was 5.01 ± 0.01, indicating its efficient delivery to the lysosomes, the ubiquitination-deficient mutant $IFNAR1^{KR}$ remained in vesicles, exhibiting a markedly higher pH_v. Remarkably, sorting of ubiquitination-competent $IFNAR1^{KR\text{-}RPT}$ mutant (see Fig. 6, A and D) was more efficient than that of $IFNAR1^{KR}$ (Fig. 4 B). These data suggest that the ubiquitination of IFNAR1 is required for routing this receptor to the lysosomes.

Expression of the lysine-less K0 ubiquitin mutant noticeably increased the number of less acidic endogenous IFNAR1-containing vesicles (Fig. S3 B), indicating that polyubiquitination is required for IFNAR1 sorting. Although expression of either

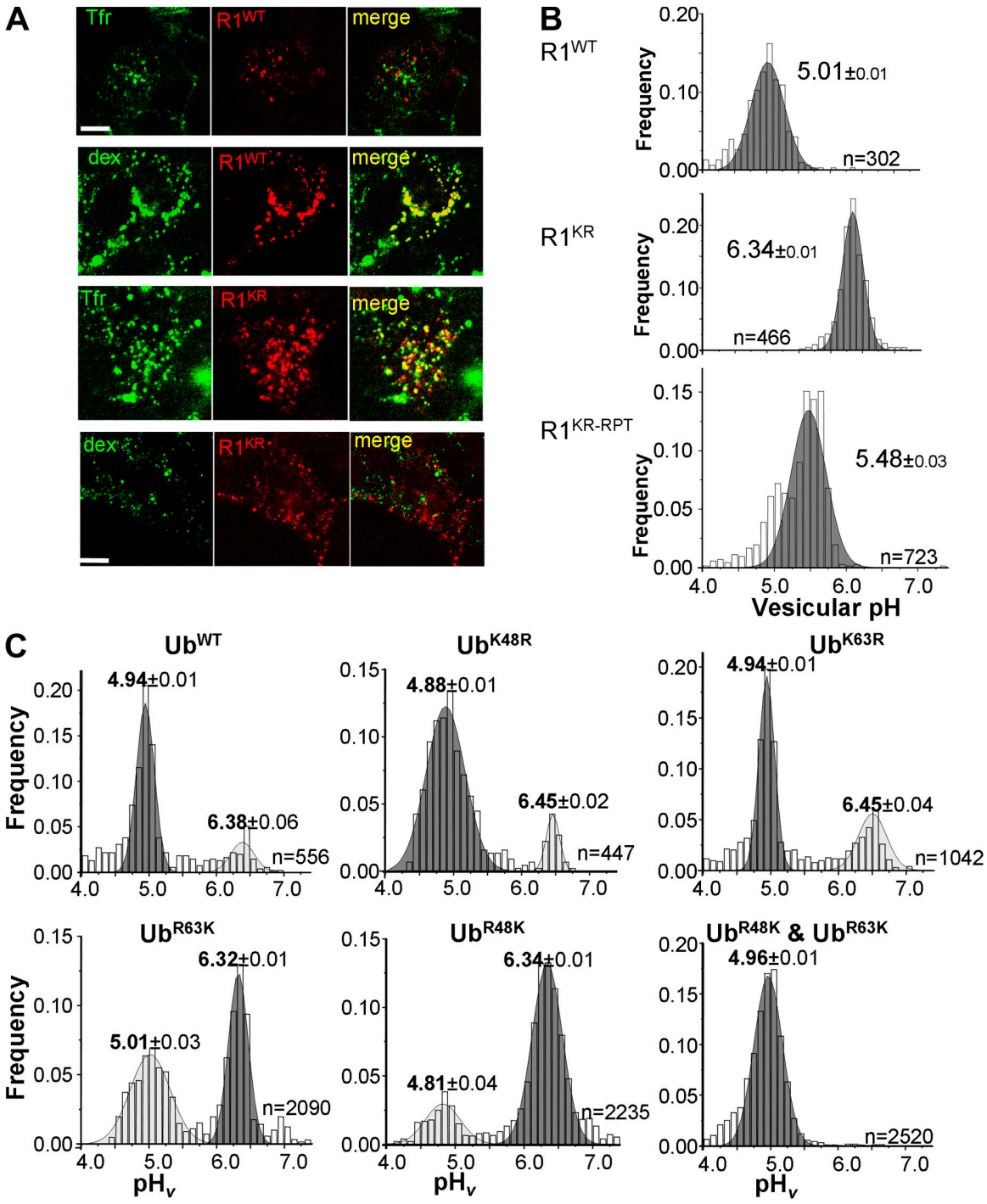

Figure 4. **Role of IFNAR1 polyubiquitination in mediating the efficient postinternalization sorting of IFNAR1.** (A) Localization of internalized Flag-tagged IFNAR1^{wt} and IFNAR1^{KR}. IFNAR1 proteins were labeled for 1 h in the presence of IFN-α, anti-Flag antibody, and TRITC-conjugated secondary Fab and were washed and chased (allowed to internalize) for an additional 30 min. Lysosomes and recycling endosomes were labeled with FITC-dextran and FITC-transferrin (Tfr), respectively. Dextran completely colocalized with Lamp1 (Fig. S2, available at http://www.jcb.org/cgi/content/full/jcb.200706034/DC1). Single optical sections of representative cells obtained by laser confocal fluorescence microscopy are depicted. A similar localization of IFNAR1^{KR} was also observed when chase time was increased to 90 min. Bars, 10 μm. (B) Vesicular pH (pH$_v$) of Flag-tagged IFNAR1-containing endosomes/lysosomes in transiently transfected HEK293T cells. Endosomal pH was measured by FRIA upon labeling and 30-min chase, and the frequency distribution of the pH$_v$ among the indicated number of analyzed vesicles (*n*) was plotted. After calibration, the ratios are expressed in pH values. A similar distribution for IFNAR1^{KR} was also observed at 90-min chase. The IFNAR1$^{KR\text{-}RPT}$ mutant contains an additional ubiquitination repeat module and is ubiquitination competent (see Fig. 6). (C) Postendocytotic sorting of Flag-tagged IFNAR1^{wt} in cells that coexpress ubiquitin constructs (as indicated, upon labeling and chase for 30 min) was monitored by pH$_v$ measurements as described in B. Data are expressed as the frequency of pH$_v$ and mean ± SEM (n = 3).

R48K or R63K alone was capable of partially reverting the sorting phenotype of K0, a combination of R48K and R63K proteins expressed together restored the efficient lysosomal sorting of IFNAR1 (Fig. 4 C).

This result could be explained by at least two possibilities. One is that, similar to IFNAR1 degradation, the sorting of IFNAR1 also requires polyubiquitin chains of both K48- and K63-linked topologies. Alternatively, given that the coexpression of R48K and R63K modestly increased IFNAR1 ubiquitination in cells compared with either of these mutants alone (Fig. 3 E), it is plausible that increased efficiency of IFNAR1 sorting could simply result from a higher overall ubiquitination of the cargo. Additional experiments revealed that expression of either K48R or K63R point ubiquitin mutants (ineffective in impeding IFNAR1 ubiquitination; Fig. 3 C) did not inhibit the efficiency of IFNAR1 sorting (Fig. 4 C) despite being expressed at high levels (Fig. S1 B), suggesting that (1) polyubiquitination via either type of chain suffices for efficient IFNAR1 delivery to lysosomes and (2) degradation defects caused by K48R or K63R ubiquitin mutants are likely caused by impaired IFNAR1 internalization.

Polyubiquitination via both K48- and K63-linked chains is required for the efficient internalization of IFNAR1

We previously demonstrated that either inhibition of βTrcp by expression of its dominant-negative $\beta Trcp^{\Delta N}$ mutant or the S535A mutation within IFNAR1 that abrogates βTrcp recruitment decreased the efficiency of endocytosis of radiolabeled IFN-α (Kumar et al., 2003). To directly determine a role of the ubiquitination of IFNAR1 in its internalization, we established a model system for assessment of the ligand-stimulated internalization of endogenous (Fig. 5 A) or exogenous (not depicted) IFNAR1 using two independent endocytosis assays (fluorescence-based and cell surface biotinylation; see Materials and methods).

The rate of IFNAR1 endocytosis was sensitive to RNAi against the clathrin heavy chain but not to treatment with the caveolae inhibitor filipin (Fig. S4 A, available at http://www.jcb.org/cgi/content/full/jcb.200706034/DC1). This rate was decreased either by knocking down βTrcp2 (short hairpin RNAs [shRNAs] against βTrcp [shBTR]; Fig. 5, B and C) or by expressing $\beta Trcp^{\Delta N}$ mutant (not depicted). Given that this delay in IFNAR1 endocytosis is already observed at 2 min (Fig. 5 B), it is likely that it reflects changes in the initial internalization receptor rather than in recycling, although the latter possibility cannot be formally excluded. This result indicates that ubiquitination of IFNAR1 might be required for the maximal rate of its endocytosis. To confirm this possibility, we used ubiquitination-deficient IFNAR1 mutants (Fig. 6 A). In line with our data, which were obtained using radiolabeled IFN-α, Ser to Ala substitution within the phosphodegron of IFNAR1 produced a mutant protein ($IFNAR1^{SA}$) that exhibited a reduced rate of internalization (Figs. 5 D and 6 E). Furthermore, another partially ubiquitination-deficient $IFNAR1^{KR}$ was also internalized less efficiently compared with wild-type IFNAR1 (Figs. 5 E and 6 F). In all, these data suggest that ubiquitination of IFNAR1 is required for its efficient internalization.

The expression of a lysine-less K0 mutant dramatically reduced the efficiency of the internalization of IFNAR1 (Fig. 5 F and Fig. S4 B) but not of transferrin receptor (not depicted), which is known to undergo ubiquitin-independent clathrin-dependent endocytosis (Hoeller et al., 2006). The latter result indicates that K0 expression does not indiscriminately affect the function of clathrin-based endocytic machinery. Intriguingly, the expression of either K48R, K63R, R48K, or R63K but not of K29R decreased the rate of IFNAR1 internalization observed in the presence of wild-type ubiquitin (Fig. 5 F and Fig. S4 C), indicating that both types of chains are essential for promoting the efficient endocytosis of IFNAR1. The higher inhibitory efficiency of K48R and K63R observed (in comparison with that of K0 or of reverse R48K or R63K mutants) is most likely the result of the higher levels of their expression (Fig. S1 B). Furthermore, although the expression of reverse R48K or R63K mutant alone also led to the inhibition of IFNAR1 internalization, the combined expression of these mutants improved the efficiency of IFNAR1 internalization almost to the level observed in cells transfected with wild-type ubiquitin (Fig. 5 F). Collectively, these results suggest that both K48- and K63-linked polyubiquitin chains are required for the efficient internalization of IFNAR1.

Both site-specific ubiquitination of IFNAR1 and integrity of a linear endocytic motif are required for efficient internalization of IFNAR1

We noted that $IFNAR1^{KR}$ mutant lacking the K501/525/526 cluster (but harboring several other lysines within its cytoplasmic tail) undergoes ubiquitination to some extent (Figs. 1 B and 6 D; Kumar et al., 2004). Nevertheless, this mutant exhibited an impaired internalization (Figs. 5 D and 6 F) and turnover (Kumar et al., 2004). Therefore, we investigated the possibility that a specific position of ubiquitin acceptor sites might play a role in IFNAR1 internalization.

The $SCF^{\beta Trcp}$ E3 ubiquitin ligase is known to preferentially conjugate ubiquitin to the lysine residues located 9–13 amino acids upstream of the ligase recognition site (Tang et al., 2003; Wu et al., 2003). These characteristics enabled us to generate IFNAR1 mutant proteins in which ubiquitination-conferring sequences (including phosphodegron and ubiquitin-accepting lysines) were copied and fused to the distal part of ubiquitination- and endocytosis-deficient $IFNAR1^{SA}$ and $IFNAR1^{KR}$, resulting in the repeat mutants, including $IFNAR1^{SA\text{-}RPT}$ and $IFNAR1^{KR\text{-}RPT}$ (Fig. 6 A). Introduction of such repeat sequence restored the ability of $IFNAR1^{SA}$ to undergo Ser phosphorylation within the phosphodegron (Fig. 6 B), to recruit βTrcp (Fig. 6 C), and to get ubiquitinated to an extent no less than that of wild-type IFNAR1 (Fig. 6 D). However, the internalization of $IFNAR1^{SA\text{-}RPT}$ mutant did not proceed faster than that of $IFNAR1^{SA}$ protein (Figs. 5 D and 6 E). Furthermore, although another $IFNAR1^{KR\text{-}RPT}$ mutant exhibited an increased Ser phosphorylation, βTrcp binding, ubiquitination, and lysosomal targeting as compared with the $IFNAR1^{KR}$ protein (Figs. 4 B and 6, B–D), the internalization rates of these mutants did not differ much and were lower compared with wild-type IFNAR1 (Fig. 6 F). Together, these results

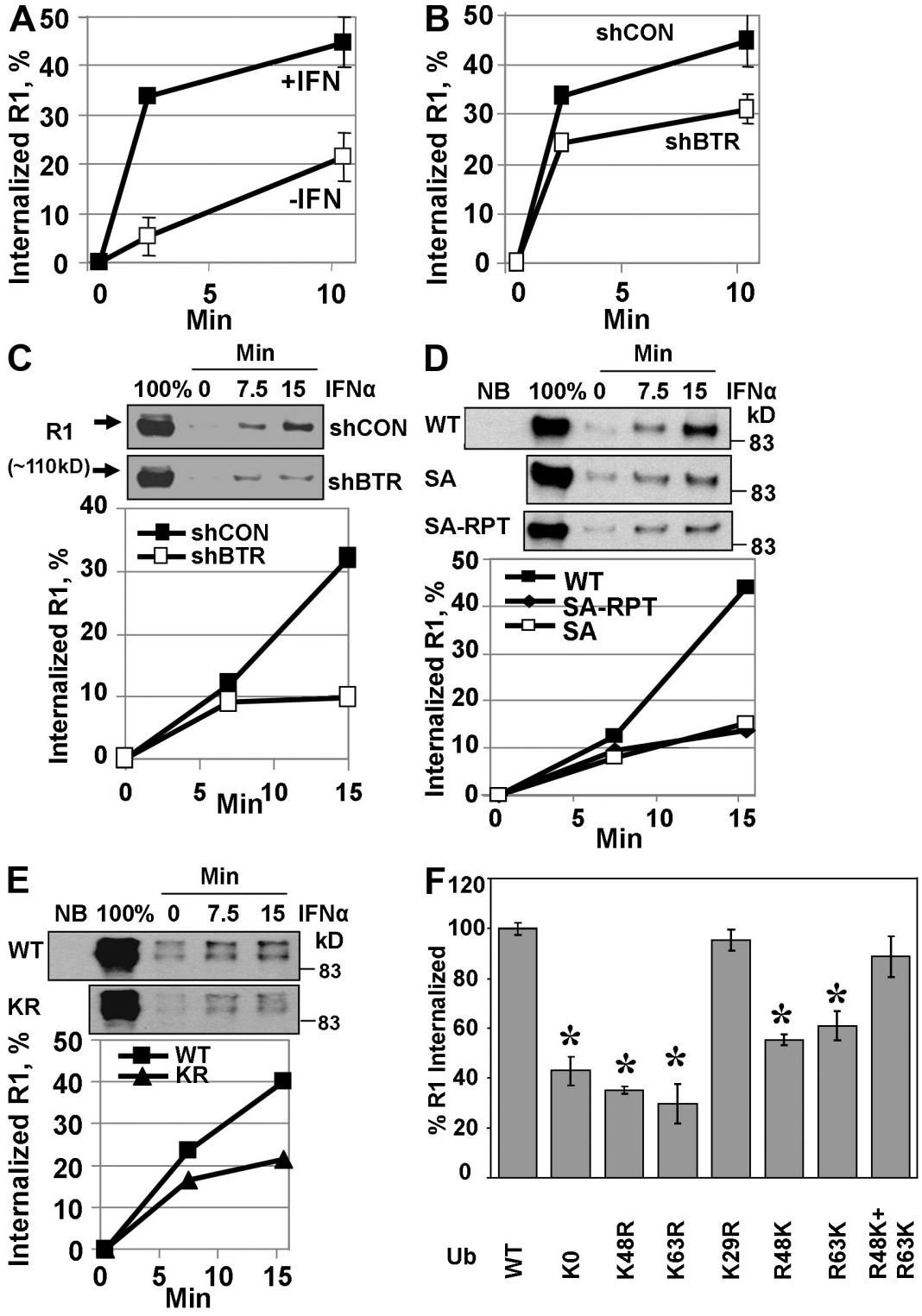

Figure 5. **Role of ubiquitination in IFNAR1 internalization.** (A) Effect of IFN-α (black squares) on the internalization of endogenous IFNAR1 measured by a fluorescence assay. All other experiments were performed in the presence of IFN-α. (B and C) Effect of βTrcp2 knockdown (shBTR) on IFNAR1 internalization observed by fluorescence assay (B; white squares) or biotinylation assay (C). (C) The internalized, biotinylated IFNAR1 analyzed by immunoblotting using anti-Flag antibody appears at the time points indicated in minutes on the top. 100% indicates the sample that represents the total amount of biotinylated IFNAR1. Quantification of these panels was calculated as (signal at time point X – signal at time point 0)/signal at 100%. (D and E) Comparison of the internalization of wild-type IFNAR1 (black squares) and its ubiquitination-deficient mutants $IFNAR1^{SA}$ and $IFNAR1^{SA\text{-}RPT}$ (D; white squares and diamonds, respectively) and $IFNAR1^{KR}$ (E; triangles) that was assessed by biotinylation assays. NB, nonbiotinylated control. (F) Effect of expression of the indicated ubiquitin mutants on the internalization of IFNAR1 assessed by fluorescent assay. Data are depicted as the percentage of IFNAR1 internalization detected in cells expressing wild-type ubiquitin (100%) at 15 min. *, $P < 0.05$ (*t* test; differences compared with wild-type ubiquitin). Error bars represent SEM.

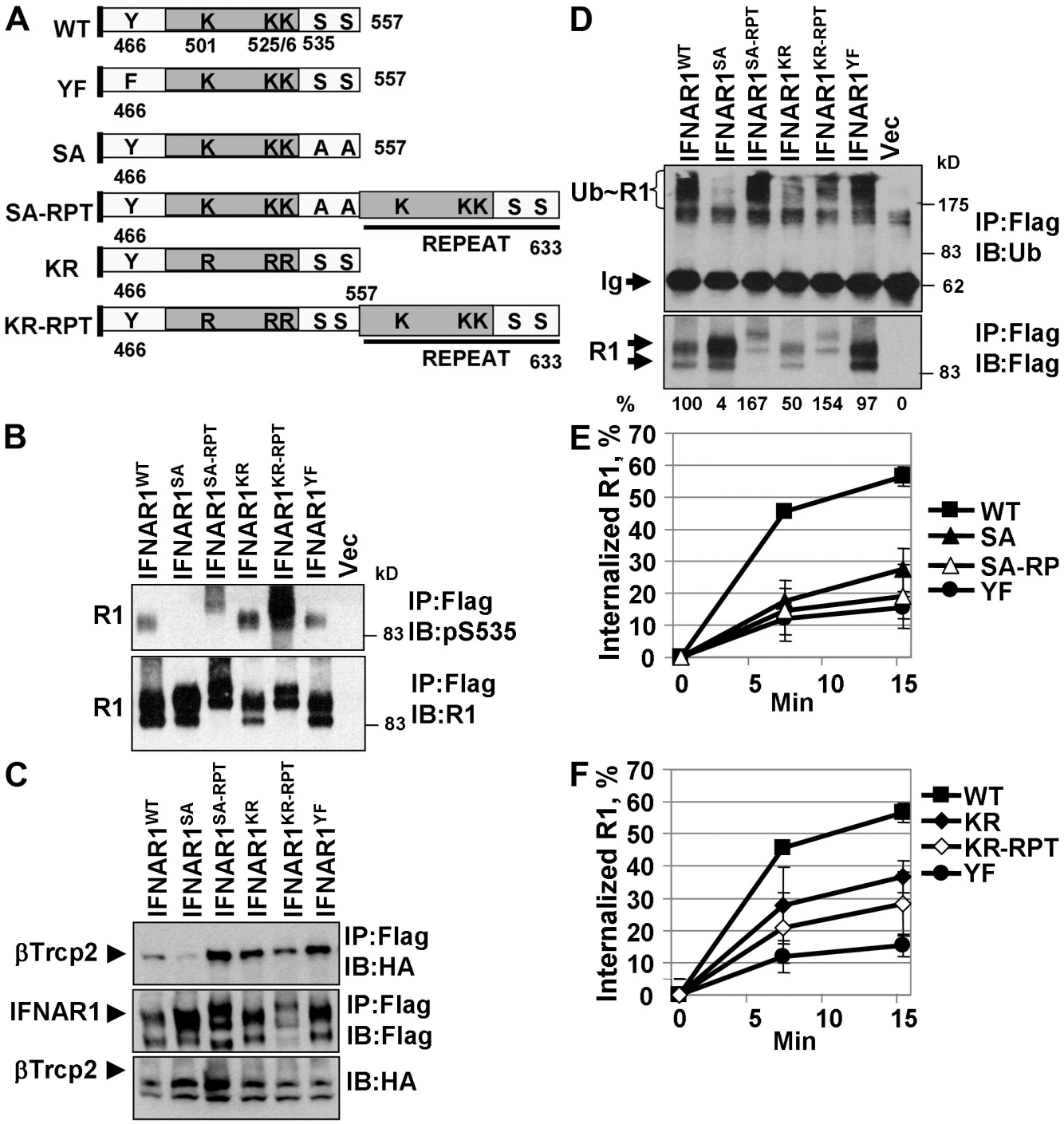

Figure 6. **Site-specific ubiquitination is required for efficient internalization of IFNAR1.** (A) Diagram of the intracellular domains of IFNAR1 proteins, including generated IFNAR1 mutants. Positions of S535 and S539 residues within the phosphodegron, of ubiquitin-acceptor cluster K501/525/526, and of Y466 within the linear endocytic motif are shown. (B) Ser535 phosphorylation of Flag-tagged IFNAR1 proteins expressed in IFN-α–treated 293T cells was analyzed by immunoblotting as in Fig. 1 F. Vec, empty vector. (C) Interaction of HA-tagged βTrcp with coexpressed Flag-tagged IFNAR1 proteins in IFN-α–treated 293T cells was analyzed by immunoprecipitation/immunoblotting using the indicated antibodies. (D) Ubiquitination of IFNAR1 proteins in IFN-α–treated 293T cells was analyzed as in Fig. 3 C. Ratios between ubiquitin and IFNAR1 signals were calculated as the percentage of such for wild-type IFNAR1. (E and F) Internalization of Flag-tagged IFNAR1 proteins was measured similar to the experiment shown in Fig. 5 A using anti-Flag antibodies. Error bars represent SEM.

suggest that the ubiquitination of IFNAR1 alone is not sufficient for conferring a maximum rate of its internalization and that the site of IFNAR1 ubiquitination may play an important role in this process.

This site specificity also indicates that some other determinants within IFNAR1 cytoplasmic tail might contribute to the rate of IFNAR1 endocytosis. Interestingly, the key lysine residues (mutated in IFNAR1^{KR}) are located within the proximity of a

Tyr-based linear endocytic motif ($_{466}$YVFF), which we found to play a role in a basal ubiquitin-independent endocytosis of IFNAR1 via interacting with AP2 (our unpublished data). Single amino acid substitution of Tyr466 to Phe within this motif resulted in an IFNAR1^{YF} protein (Fig. 6 A) that exhibited grossly impaired internalization (Figs. 6, E and F; and 7 A) despite being competent in Ser535 phosphorylation, recruitment of βTrcp, and ubiquitination (Fig. 6, B–D). Furthermore, while undergoing efficient ubiquitination, IFNAR1^{YF} mutant degraded much slower than wild-type IFNAR1 (Fig. 7 B). These results confirm that ubiquitination is not sufficient for rapid IFNAR1 internalization and turnover, suggesting that the linear endocytic motif plays a key role in these processes.

Tyr-based linear endocytic motifs are known to serve as a recognition site for the AP50 subunit of the AP2 complex (for review see Bonifacino and Traub, 2003). Immunoprecipitated from ligand-treated cells, the IFNAR1^{YF} mutant did not efficiently interact with coexpressed AP50. These data indicate that binding of AP50 to IFNAR1 is mainly mediated by a linear motif rather than by receptor ubiquitination. Remarkably, endocytosis-deficient IFNAR1^{SA} and IFNAR1^{KR} mutants that contain the unmodified Tyr-based motif exhibited a noticeably decreased interaction with AP50 (Fig. 7 C) that was proportional to the extent of their ubiquitination (Fig. 6 D). This result suggests that IFNAR1 ubiquitination might be required for exposure of the Tyr-based motif to AP2 components.

Indeed, although a brief treatment of cells with IFN-α stimulated the interaction between endogenous IFNAR1 and AP50, inhibition of IFNAR1 ubiquitination by expressing either dominant-negative βTrcp$^{\Delta N}$ mutant or shRNA against βTrcp2 decreased this interaction (Fig. 7 D). Furthermore, the expression of either K0, K63R, or K48R (but not K29R) ubiquitin mutants also decreased the ligand-induced recruitment of AP50 to endogenous IFNAR1 (Fig. 7 E). Finally, RNAi-mediated knockdown of an AP2 subunit (α2) led to a noticeable decrease in the rate of internalization of endogenous IFNAR1 (Fig. 7 F). Together, these data suggest that ubiquitination of IFNAR1 is required for efficient exposure of the Tyr-based linear endocytic motif within IFNAR1 to the interaction with AP2, which is essential for achieving the maximum rate of IFNAR1 internalization.

Discussion

Interaction between ubiquitination and the linear endocytic motif in internalization of IFNAR1

Current paradigm on the role of ubiquitination in the endocytosis of cell surface receptors proposes that ubiquitinated cargo (often monoubiquitinated) is recognized by the ubiquitin-binding domain–containing adaptor proteins. These proteins tether this cargo to the components of endocytic and sorting machinery, thereby enabling receptor internalization and postinternalization sorting. Within the original model, internalization or sorting could be triggered simply by a linear fusion of ubiquitin to the intracellular tail of a receptor. This suggests that neither polyubiquitination, the topology of ubiquitin chains, nor the site of ubiquitin conjugation should be important for the efficiency of endocytosis (Dikic, 2003; Haglund et al., 2003a; Hicke and Dunn, 2003; Polo et al., 2003; Raiborg et al., 2003; Sigismund et al., 2004).

In this study, we report that IFNAR1 undergoes polyubiquitination via both K48- and K63-linked chains. Although an efficient internalization of IFNAR1 requires both types of these chains, once the receptor is internalized, its postinternalization fate depends on polyubiquitination that does not discriminate between K48- and K63-linked chains. This diverse ubiquitination type requirement indicates that IFNAR1 internalization and IFNAR1 postinternalization sorting use differential mechanisms by which ubiquitination regulates these events.

Remarkably, a conjugation site-specific polyubiquitination of IFNAR1 is required but not sufficient for the maximum rate of IFNAR1 internalization, which also depends on the integrity of a linear Tyr-based endocytic motif. Interfering with either K48/K63 linkages or the ubiquitination of IFNAR1 decreases the interaction between this receptor and components of the adaptin complex, which is essential for efficient IFNAR1 internalization. Collectively, our data suggest that ubiquitination of IFNAR1 on specific ubiquitin-acceptor lysines might unmask a Tyr-based linear endocytic motif for its interaction with the adaptin components under conditions permitting both K48- and K63-linked ubiquitin chains. Such ubiquitination-dependent exposure of a linear endocytic motif to increase the endocytic rate represents a novel paradigm on a role of ubiquitin in regulating the endocytosis of signaling receptors.

Putative mechanisms for ubiquitin-dependent exposure of an endocytic motif within IFNAR1 and its significance for endocytosis

Several models might explain how site-specific ubiquitination contributes to interaction between the linear motif within IFNAR1 and the adaptin complex, which is required for the efficient internalization of IFNAR1. In the absence of the ligand, either an intramolecular interaction or a putative IFNAR1-interacting protein complex might shield a Tyr-based linear motif and prevent it from interacting with the AP50 subunit. Upon IFN addition, a yet unknown protein kinase phosphorylates IFNAR1 within its phosphodegron on Ser535 and Ser539 (Kumar et al., 2004; Marijanovic et al., 2006). This phosphorylation enables recruitment of the SCF$^{\beta Trcp}$ E3 ubiquitin ligase that facilitates the ubiquitination of IFNAR1 on various lysines, including a cluster of K501, K525, and K526 (Kumar et al., 2003, 2004).

This site-specific ubiquitination of IFNAR1 results in exposure of the linear motif to AP50. This exposure might occur via altering the conformation of IFNAR1 intracellular tail or/and rearranging a putative masking protein complex. The latter scenario is based on exciting discoveries that many proteins can interact with ubiquitin moieties either via bona fide specialized ubiquitin-interacting domains (French et al., 2005; Seet et al., 2006) or via specific subtypes of other domains such as coil-coiled, LZ, novel zinc finger (Kanayama et al., 2004; Ea et al., 2006), and SH3 domains (Stamenova et al., 2007). Whereas additional mechanisms leading to an exposure of a linear endocytic motif cannot be ruled out, ubiquitination-stimulated

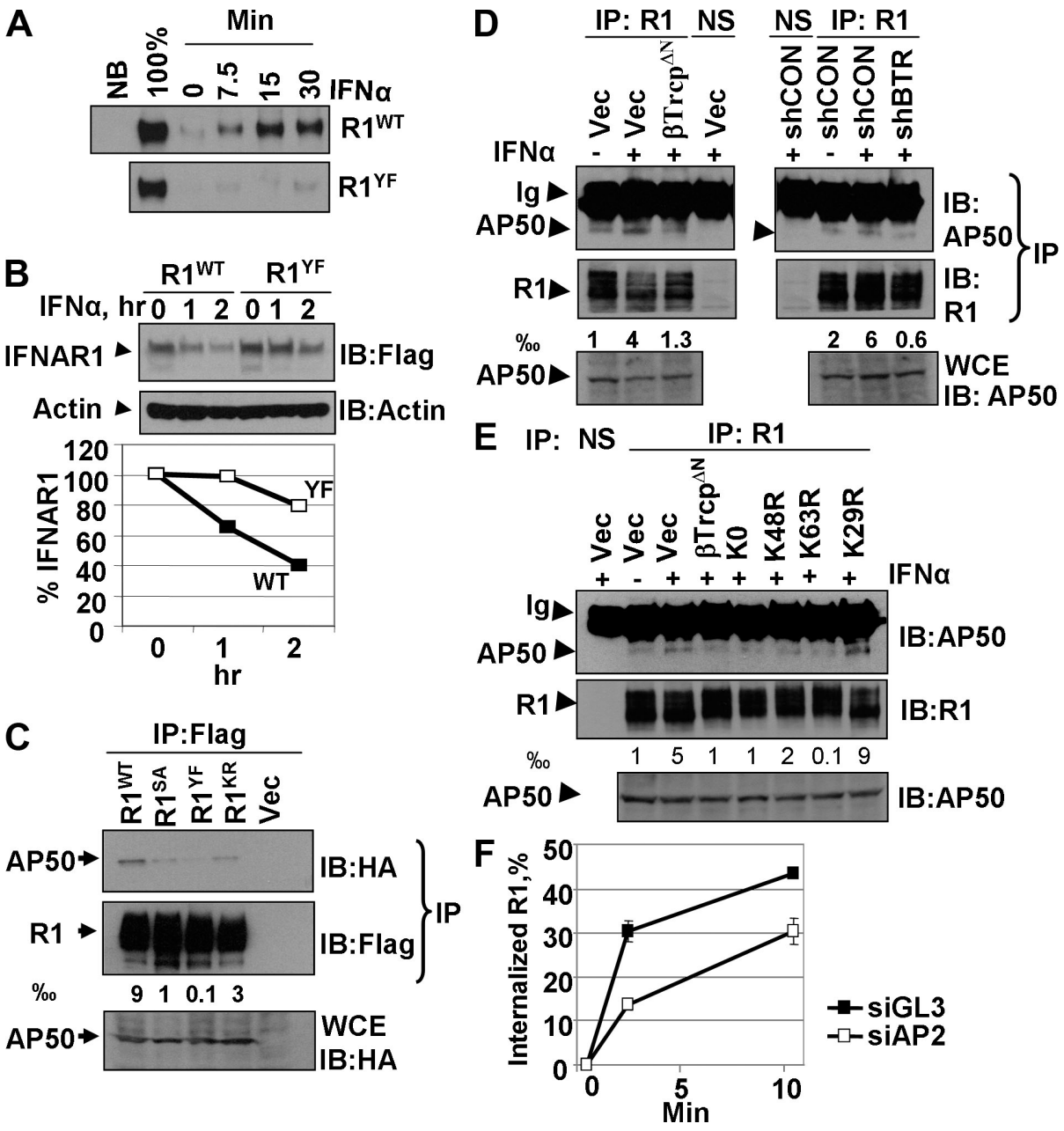

Figure 7. **Cooperation between IFNAR1 ubiquitination and exposure of the linear Tyr-based endocytic motif.** (A) Internalization of IFNAR1^{wt} and IFNAR1^{Y466F} was assessed by biotinylation assay as in Fig. 5 D. (B) Degradation of the indicated IFNAR1 proteins was analyzed by cycloheximide chase as in Fig. 2 C. (C–E) Interaction of endogenous (C) or exogenous (D and E) IFNAR1 proteins with AP50 under the indicated conditions was analyzed by immunoprecipitation/immunoblotting using the indicated antibodies. The fraction of AP50 bound to IFNAR1 (calculated as a thousandth) is shown. NS, immunoprecipitation with irrelevant nonspecific monoclonal antibody. (F) Effect of AP2 knockdown on the internalization of endogenous IFNAR1 was analyzed as in Fig. 5 B. Control siRNA (siGL3) were targeted against luciferase. Error bars represent SEM.

interaction of the AP2 adaptin complex with such a motif on one hand and clathrin lattices on the other hand should promote the efficient internalization of IFNAR1.

Future studies will identify the nature of masking the linear endocytic motif in the absence of ubiquitination. A candidate regulator of such a phenomenon is a Janus kinase, Tyk2, whose interaction with IFNAR1 prevents its ligand-independent endocytosis in a catalytic-independent manner (Ragimbeau et al., 2003). Although we found that Tyk2 inhibits ligand/ubiquitination-independent internalization of IFNAR1 via masking the linear endocytic motifs (including a Tyr-based motif; our unpublished data), a dissociation of Tyk2 from IFNAR1 under the conditions of ligand treatment described in Fig. 7 (D and E) was not observed in this study (our unpublished data).

In addition, the catalytic function of Jak kinases and counterpart protein phosphatases that determine the phosphorylation status of the Tyr residues within IFNAR1 (including Y466; Yan et al., 1996) might add another level of regulation complexity. Phosphorylation of Y466 is expected to reduce the affinity of AP50 for the Tyr-based endocytic motif as described for CTLA-4

(Chuang et al., 1997; Shiratori et al., 1997; Zhang and Allison, 1997). Thus, it is possible that tyrosine phosphatase activities play a role in regulating IFNAR1 endocytosis (indeed, the overexpression of tyrosine phosphatase PTP1B stimulates IFNAR1 internalization; unpublished data). Further investigation is underway of this modification as well as of proteins that interact with Tyk2 and ubiquitinated versus nonubiquitinated IFNAR1 and that might regulate IFNAR1 endocytosis and degradation.

Diverse topology of ubiquitin chains and their requirement for the internalization of IFNAR1

Whereas the $SCF^{\beta Trcp}$ E3 ubiquitin ligase is well known to facilitate the K48-linked polyubiquitination of numerous proteasomal substrates (Harper et al., 2002; Fuchs et al., 2004; Petroski and Deshaies, 2005), our data demonstrate that IFNAR1 is ubiquitinated by K63-linked chains as well. Although we cannot rule out that an additional E3 produces the latter chains on IFNAR1 in vivo, purified $SCF^{\beta Trcp}$ in combination with Cdc34 can actually produce both types of linkages in vitro (Fig. 1 C), and the efficiency of these reactions is proportional to the levels of specific linkages present on IFNAR1 in cells (Fig. 1 B). Intriguingly, other ubiquitin ligases of both HECT and RING superfamilies (such as yeast Rsp5 and mammalian c-Cbl) were implicated in the degradation of both lysosomal (such as uracil permease and EGFR; Hicke and Dunn, 2003) and proteasomal (such as Mga2p120 [Shcherbik et al., 2003] and Syk [Rao et al., 2001]) substrates.

It remains unclear what factors would determine the specificity of polyubiquitin linkages present on IFNAR1. It is plausible that recruitment of specific E2 in cells would serve as such a determinant. Although some of our in vitro studies were performed using a notoriously promiscuous UbcH5c (Brzovic and Klevit, 2006), which is known to produce non–K48-linked chains when combined with recombinant Cul1 and Roc1 in vitro (Wu et al., 2002), we observed a similar result using a more specific Cdc34, albeit the latter formed K63-linked chains with lesser efficiency (Fig. 1 C). Other contributing factors may include special substrate constraint or a lack thereof (for example, cytoplasmic- or membrane-bound localization of a substrate) as well as the extent of Cul1 modification by Nedd8.

Future studies will determine why both types of polyubiquitin chains are needed for efficient IFNAR1 internalization and turnover. Although our mass spectrometry data are consistent with analyses using ubiquitin mutants, the current state of technology does not allow us to directly address this issue because we cannot distinguish whether the effect of the ubiquitin mutants is mediated solely by the altered ubiquitination of IFNAR1 itself or by other potential regulators. On one hand, the possibility that mixed topology K48/K63 chains are actually conjugated to the same ubiquitin-acceptor lysines of IFNAR1 in a random fashion to mediate specific functions of the unmasking linear motif is counterintuitive. On the other hand, our previous data showing that mutation of either K501 or K525/526 alone does not substantially affect IFNAR1 degradation (Kumar et al., 2004) raise doubts about a notion that these key Lys residues within the IFNAR1 cluster are decorated alternatively by either K63- or K48-linked chains to target different components of an IFNAR1-binding complex. Another possibility is that although the K63-linked chain (conjugated to IFNAR1) titrates away a putative masking protein, the expression of K48R interferes with the proteasomal degradation of such a protein, thereby saturating K63-dependent binding and preventing exposure of the linear motif to AP50. Intriguingly, although a decrease in internalization of growth hormone receptor in cells treated with proteasomal inhibitors has been previously reported (van Kerkhof et al., 2000), such treatment did not affect IFNAR1 internalization (our unpublished data).

Role of ubiquitination in receptor internalization

As per the role of ubiquitination, linear motifs, or both in clathrin-mediated internalization of cell surface receptors, three groups of receptors could be envisioned. The first group includes receptors whose linear motifs are required and sufficient for rapid internalization (for example, transferrin receptor). The second group includes those receptors whose ubiquitination is required and sufficient for the maximal rate of internalization. In keeping with the well-established fact that any kind of ubiquitination should provide a substrate receptor with an endocytic signal (Hicke and Dunn, 2003), a properly ubiquitinated $IFNAR1^{YF}$ mutant still undergoes internalization at a noticeable rate (Figs. 6 F and 7 A). These results indicating that the ubiquitination of IFNAR1 is sufficient for some extent of internalization are in line with reports on chimerical proteins that harbor ubiquitin fusion instead of a cytoplasmic tail (Haglund et al., 2003b; Barriere et al., 2006). Further studies will determine other endogenous proteins that undergo clathrin-dependent internalization solely via the ubiquitin-mediated pathway. Additional complexity is constituted by the existence of ubiquitin-dependent but clathrin-independent mechanisms of receptor internalization (Sigismund et al., 2005).

Cooperation between ubiquitination and linear endocytic motifs might serve as a mechanism for promoting internalization of the third group of cell surface receptors, including IFNAR1. Whereas ubiquitination appears to affect the function of the linear motif within IFNAR1, these two pathways could work simply in an additive manner for some other receptors to ensure their robust internalization. Given that different receptors interacting with their own binding proteins may harbor different linear motifs within diverse structural contexts, it is not surprising that various individual receptors might require different types of ubiquitination (multiple mono- versus polyubiquitination of various chain topologies) for maximal efficiency of endocytosis as reported above (see Introduction).

Our observations presented here are limited to the role of protein ubiquitination in the recognition of linear determinants (within a substrate of ubiquitination) that occurs during endocytosis. However, given that ubiquitination is also implicated in regulating other types of protein trafficking (e.g., in the nuclear export of p53; Li et al., 2003), it is tempting to speculate about a possible interaction between ubiquitination and linear trafficking signals that might use a similar mechanism to modulate the efficiency of protein transport between different subcellular compartments. Future studies are required to test this possibility.

Materials and methods

Cells and constructs

HEK293T cells were maintained and transfected as described previously (Fuchs et al., 1999). Vectors for the expression of HA- or myc-tagged βTrcp2 (wild-type or dominant-negative $\beta Trcp^{\Delta N}$; Fuchs et al., 1999; Winston et al., 1999), C-terminal Flag-tagged human IFNAR1 (Kumar et al., 2003), HA-ubiquitins (Mosesson et al., 2003), and HA-AP50 (Rohde et al., 2002) were previously described. Human IFNAR1 with Flag tag inserted after the signal sequence at the N terminus was constructed by an overlap PCR method. All IFNAR1 mutations created by PCR and site-directed mutagenesis were verified by DNA sequencing. Reagents for RNAi approach, including shRNA constructs for knocking down the heavy chain of clathrin (Royle et al., 2005) or βTrcp2 (Li et al., 2004), as well as siRNA oligonucleotides for knocking down the α subunit of the AP2 complex (Barriere et al., 2006) were characterized and described previously. Control shRNA and siRNA were targeted against GFP (Jin et al., 2003) and luciferase (Kumar et al., 2003), respectively.

Antibodies, immunotechniques, and ubiquitination assays

Antibodies were purchased against Flag (M2; Sigma-Aldrich), HA (HA11; Covance), myc-tag, β-actin, and c-Jun (Santa Cruz Biotechnology, Inc.), AP50 (μ2; BD Transduction Laboratories), and ubiquitin (FK2; BIOMOL International, L.P.). Antibodies that recognize endogenous IFNAR1 (Goldman et al., 1999) and IFNAR1 phosphorylated on Ser535 (pS535; Kumar et al., 2004) were described previously. Secondary antibodies conjugated to HRP were purchased from Chemicon and Invitrogen. Immunoprecipitation and immunoblotting procedures were described previously (Fuchs et al., 1999). Densitometry data were obtained, analyzed, and quantitated using Image software (version Beta 4.0.2; Scion), and the digital images were prepared using Photoshop 7.0 software (Adobe).

In vitro ubiquitin ligation assay was performed as previously described (Tan et al., 1999) using recombinant $SCF^{\beta Trcp}$ and either UbcH5c or Cdc34 (gifts of Z.-Q. Pan, Mount Sinai School of Medicine, New York, NY) as E2. In brief, $SCF^{\beta Trcp}$ E ligase was incubated with E1, E2, ATP, and biotin-labeled ubiquitins (wild type, R48K, and R63K as indicated; Boston Biochem). After 1-h incubation at 37°C, the reaction was terminated by adding SDS-PAGE loading buffer, and ligase was boiled, separated on 10% SDS-PAGE, and transferred to polyvinylidene difluoride membrane. The blot was blocked with 3% BSA in TBS, incubated with Avidin-HRP, and developed by chemiluminescence.

In vivo ubiquitination was performed as described previously (Kumar et al., 2004). In brief, 293T cells in 10-cm dishes were cotransfected with 1 μg Flag-tagged IFNAR1 or empty vector with 4 μg of various HA-tagged ubiquitin plasmids (where indicated). 36 h after transfection, cells were harvested and lysed under denaturing conditions (1% SDS). Upon neutralization of SDS with 10 vol of 1% Triton X-100, IFNAR1 was immunoprecipitated with anti-FLAG antibody (when cotransfected with FLAG-IFNAR1 plasmids) or with anti-IFNAR1 antibody (when cotransfected with empty vector) and analyzed by immunoblotting with the indicated antibodies. Where indicated, the relative percentage of ubiquitination was calculated by setting the ratio of ubiquitination with wild-type IFNAR1 or wild-type ubiquitin as 100%.

Mass spectrometric analysis of polyubiquitin chains linked to IFNAR1

Flag-tagged IFNAR1 proteins (wild type or KR mutant) were expressed in 293T cells and purified using M2 agarose (Sigma-Aldrich) followed by sequential stringent washes with buffers containing 1% Nonidet P-40, 1 M NaCl, and 0.1% SDS. Subsequent washes were performed with the same buffer containing 200 mM NaCl, 100 mM NaCl, and, finally, TBS. These washes were stringent enough to remove any detectable Tyk2 from immunoprecipitated IFNAR1. The precipitated proteins were eluted with 0.1 M glycine, pH 3.0 and resolved by SDS-PAGE. Approximately 1% of the eluate was analyzed by immunoblotting with antiubiquitin antibody (FK2; BIOMOL International, L.P.) to determine the apparent molecular weight of ubiquitinated receptor and anti-FLAG M2 antibody. 80% of eluate was analyzed by SDS-PAGE followed by colloidal Coomassie (Invitrogen) staining.

Gel slices containing the ubiquitinated receptor and the corresponding region in vector control lane from the Coomassie-stained gel were used for the analysis of polyubiquitin linkages according to previously established methods (Kirkpatrick et al., 2006; Xu and Peng, 2006). In brief, the proteins in the gel slices were digested by trypsin with the addition of eight stable isotope-labeled peptides as internal standards, including all seven –GG peptides and one Ub peptide (Thr55-Lys63). The resulting peptide mixtures were analyzed by reverse-phase liquid chromatography–tandem mass spectrometry on a hybrid mass spectrometer (LTQ-Orbitrap; Thermo Fisher Scientific). The instrument was operated to monitor the eight peptides and their related native counterparts by selective reaction monitoring. Quantification analysis was performed using Xcalibur software (Thermo Fisher Scientific). Additional sequencing of all identified peptides and calculation of the protein abundance index revealed that the vast majority of these peptides originated from either ubiquitin or IFNAR1 itself (Table S1, available at http://www.jcb.org/cgi/content/full/jcb.200706034/DC1).

IFNAR1 internalization

Two different assays were used for measuring the rate of IFNAR1 internalization: fluorescence-based assay and cell surface reversible biotinylation assay. The fluorescence-based assay determines the internalization of IFNAR1 by measuring the loss of cell surface immunoreactivity of epitope-tagged or endogenous receptors using an ELISA assay as described previously (Barriere et al., 2006) with the following modifications. In brief, 293T cells in 60-mm dishes were transfected (where indicated) and plated onto 24-well plates. Transfection of shRNAs against clathrin heavy chain (2 μg of plasmids) or the α-adaptin subunit of AP2 complex (100 nM oligonucleotides) were performed twice in 24-h intervals and analyzed after 72 h. Cells were starved for 2 h in serum-free DME and chilled on ice for 15 min. Internalization was initiated by the incubation of cells with warm (37°C) serum-free DME containing IFN-α for the indicated time periods at 37°C, or cells were kept on ice without adding IFN-α (time point 0) and terminated by placing the plate on ice. Cells were washed, blocked, and incubated with anti-IFNAR1 antibody (AA3 for endogenous IFNAR1) or anti-FLAG antibody (monoclonal Flag M2 for exogenous IFNAR1 and its mutants; Sigma-Aldrich) for 1 h, washed, and incubated with HRP-conjugated goat anti–mouse secondary antibody (Invitrogen) for 1 h. After extensive washing, cells were incubated with AmplexRed Ultra Reagent (10-acetyl-3,7-dihydroxyphenoxazine; Invitrogen). Aliquots were transferred to black 96-well plates, and fluorescence was measured by reading with a fluorescence plate reader (Chameleon; BIOSCAN) using 530-nm filters for excitation and 590-nm filters for emission. Results were calculated using the following formula: % Internalized $= [1 - (V_s - V_b)$ at $t_n/(V_s - V_b)$ at $t_0] \times 100$, in which V_s is the value of samples, V_b is the value of background (mock transfected or nonspecific antibody), t_n is time point n, and t_0 is time point 0. Average results of at least four experiments (each in triplicates) ± SEM are presented.

Cell surface biotinylation was performed as described previously (Hammond et al., 2003). This assay uses immunoblotting analysis to detect biotinylated proteins that were protected from debiotinylation as a result of their internalization. In brief, 293T cells in 60-mm dishes were transfected with 0.1 μg of various C-terminal 3×-Flag–tagged IFNAR1 plasmids and 1.9 μg pCDNA3 or other indicated plasmids. 36 h after transfection, cells were starved in serum-free DME for 2 h, chilled on ice, and washed with PBS. Surface biotinylation was performed with 0.25 mg/ml EZ-Link-Sulfo-NHS-S-S-biotin (Thermo Fisher Scientific) in 150 mM $Na2B4O7$, pH 8.0, for 15–30 min on ice. After quenching the excess unreacted biotin by washing three times with DME containing 0.1% BSA followed by an additional wash with ice-cold Hepes-buffered saline (HBS; 10 mM Hepes-NaOH, pH 7.4, 150 mM NaCl) containing 0.7 mM $CaCl_2$ and 0.5 mM $MgCl_2$ (HBS^{2+}), cells were either kept on ice or incubated at 37°C after adding warm DME containing IFN-α to allow internalization at the indicated time points. After internalization, cells were returned to ice and were either left untreated (100%) or subjected to three 20-min incubations with 100 mM sodium 2-mercaptoethanesulfonic acid (MESNA; Sigma-Aldrich) in 50 mM Tris-HCl, pH 8.6, 100 mM NaCl, 1 mM EDTA, and 0.2% BSA to selectively remove biotin remaining at the cell surface. Time point 0 was set using cells that were biotinylated and kept on ice and treated with MESNA to remove surface biotin. Cells that were not biotinylated were used as a negative control. Cells were then rinsed twice with HBS^{2+} and residual MESNA quenched by 10-min incubation with ice-cold 120 mM iodoacetamide in HBS^{2+}. After two additional washes with ice-cold HBS, cells were lysed with 60 mM *n*-octyl β-D-glucopyranoside (Thermo Fisher Scientific) and 0.1% SDS in the same buffer containing protease inhibitor cocktail for 10–20 min and were centrifuged at 15,000 rpm for 15 min. Biotinylated proteins were recovered by incubating with immobilized NeutrAvidin (Thermo Fisher Scientific) overnight, and proteins were washed, boiled with SDS-PAGE loading buffer, separated on 10% SDS-PAGE, and analyzed by immunoblotting with anti-Flag M2 antibody to detect Flag-tagged IFNAR1. Densitometry data were obtained and analyzed using Image software. Results were expressed as the percentage internalized to total biotinylated receptor (after subtracting the value at time point 0). Representative results of three independent experiments are shown.

IFNAR1–AP2 interactions

For detecting endogenous AP50 interaction with IFNAR1, four 10-cm plates of 293T cells at 60–70% confluence were either mock transfected or transfected with various constructs (shRNA against βTrcp2 or GFP, pEF-βTrcp2$^{\Delta N}$, ubiquitin constructs, or empty vector; 4 μg/plate). 48 h after transfection, cells were starved in serum-free DME containing 20 mM methylamine hydrochloride for 3 h. Cells were chilled on ice for 15 min and stimulated or not stimulated with 1,500 IU/ml IFN-α for 2.5 min at 37°C. Cells were washed with ice-cold PBS, harvested, and collected by centrifugation at 3,000 rpm for 5 min, and the pellets were lysed using TGH lysis buffer (1% Triton X-100, 10% glycerol, 50 mM Hepes, pH 7.4, 1 mM EGTA, 50 mM NaCl, 1 mM sodium orthovanadate, 1 mM PMSF, 544 μM iodoacetamide, and protease inhibitor cocktail) by rotating at 4°C for 1 h. After centrifugation at 14,000 rpm for 30 min, lysates were precleared with 30 μl of protein A beads for 2 h. Lysates were incubated with EA12 antibody for 3 h followed by 50 μl of protein A beads overnight at 4°C, and lysates were washed with lysis buffer four times, boiled with SDS-PAGE loading buffer, separated by 10% SDS-PAGE, and transferred to a polyvinylidene difluoride membrane. The blot was probed with AP50 antibody to detect AP50 and with GB8 antibody to detect IFNAR1. Whole cell lysates were analyzed for the expression of AP50. Representative results of four independent experiments are shown.

For interactions of exogenous IFNAR1 with AP50, 293T cells were transfected with 3 μg N-terminal Flag-tagged IFNAR1, 2 μg HA-tagged AP50, and 0.25 μg HA-tagged Tyk2 (to prevent ligand-independent internalization of IFNAR1; Ragimbeau et al., 2003). 48 h after transfection, cells were starved in serum-free DME containing 20 mM methylamine hydrochloride for 3 h. Cells were harvested using cell dissociation buffer (enzyme-free Hank's based; Invitrogen), incubated with anti-Flag antibody (M2; Sigma-Aldrich) for 3–4 h, and stimulated with 1,500 IU/ml IFN-α for 2.5 min by incubating at 37°C. Cells were washed thoroughly with 1× PBS and pelleted by centrifugation at 3,000 rpm for 5 min. Pellets were lysed with TGH lysis buffer. Lysates were incubated with protein A beads overnight, and the beads were washed with lysis buffer. After boiling with SDS-PAGE loading buffer, an aliquot from each sample was separated on 10% SDS-PAGE and analyzed for IFNAR1 levels by Flag immunoblotting to normalize the receptor levels. Based on normalization, adequate amounts of samples were separated on 10% SDS-PAGE and analyzed by immunoblotting with anti-HA antibody to detect AP50 and anti-Flag antibody to detect IFNAR1. Whole cell lysates were analyzed for the expression of HA-AP50. Representative results of three independent experiments are shown.

Vesicular pH (pH_v) measurement, microscopy, and image acquisition

For transient transfection of 293T, cells was performed with Lipofectamine 2000 (Invitrogen) according to the manufacturer's recommendations and analyzed after 48 h. For cotransfection, the cDNA ratio of Ub/IFNAR was 4:1. To monitor the endocytic trafficking of internalized IFNAR1 chimeras, the pH_v of cargo-containing vesicles was determined by FRIA in 293T cells essentially as described for cystic fibrosis transmembrane conductance regulator using the appropriate primary and FITC-conjugated secondary Fab. In brief, after 48-h transient transfection, cell surface IFNAR1 proteins were labeled with primary antibody (Flag-M2; 1/100; Sigma-Aldrich) and FITC-conjugated goat anti–mouse secondary Fab (1/200; Jackson ImmunoResearch Laboratories) by incubating simultaneously for 1 h at 37° in the presence of 6,000 U/ml IFN-α. Cells were washed with Na/KCl medium (140 mM NaCl, 5 mM KCl, 20 mM Hepes, 10 mM glucose, 0.1 mM $CaCl_2$, and 1 mM $MgCl_2$, pH 7.3) and chased for an additional 30 min at 37°C. Additional experiments for internalization-deficient mutants were also performed using the chase time of 90 min. Fluid-phase secondary antibody uptake was undetectable by FRIA in mock-transfected cells.

FRIA was performed on an inverted fluorescence microscope (Axiovert 100; Carl Zeiss, Inc.) at 35°C equipped with a cooled CCD camera (ORCA-ER 1394; Hamamatsu) and a plan Achromat 63× NA 1.4 objective at 25°C. Fluorescence ratio image acquisition and analysis were performed with MetaFluor software (MDS Analytical Technologies). Images were acquired at 490 ± 5- and 440 ± 10-nm excitation wavelengths using a 535 ± 25-nm emission filter. In situ calibration was performed by clamping the vesicular pH between 4.5 and 7.4 in K^+-rich medium (135 mM KCl, 10 mM NaCl, 20 mM Hepes or 20 mM MES, 1 mM $MgCl_2$, and 0.1 mM $CaCl_2$) in the presence of 10 μM nigericin and 10 μM monensin (Sigma-Aldrich) and recording the fluorescence ratio of FITC-Fab antibody. Calibration curves, which were generated by fluorescence ratio values as a function of extracellular pH, served to calculate the luminal pH of individual vesicles after fluorescence background subtraction at both excitation wavelengths. Calibration of colocalization with early/late vesicle markers was assessed (Fig. S2). Verification that antibody binding is not disturbed by physiologic lysosomal pH was also performed (Fig. S3 A). In each experiment, the pH_v of 200–700 vesicles was determined. As an internal control, one point calibration was performed on each coverslip by clamping the pH_v to 6.5 in the presence of monensin and nigericin. Mono- or multipeak Gaussian distributions of pH_v values were obtained with Origin 7.0 software (OriginLab Corporation). The mean pH_v of each vesicle population was calculated as the arithmetic mean of the data and was identical to the Gaussian mean based on single-peak distribution fitting. Three independent experiments were performed for each condition.

For immunofluorescence microscopy, 293T cells were plated on poly-Lys–coated coverslips 24 h before experiments. Lysosomes were labeled overnight in the presence of 50 μg/ml FITC-dextran (mol wt of 10 kD; Invitrogen) and were chased for >3 h. Recycling endosomes were visualized with 5 μg/ml FITC-Tf (1-h labeling at 37°C) and chased for 15 min. Cells expressing IFNAR1 were allowed to internalize Flag M2 antibody (1/100) complexed to TRITC-conjugated goat anti–mouse IgG (for 45 min at 37°C) in DME supplemented with 10% FBS and were chased as described for pH_v measurement. Single optical sections were collected by a laser confocal fluorescence microscope (LSM510; Carl Zeiss, Inc.) equipped with a plan Apochromat 63× NA 1.4 objective (Carl Zeiss, Inc.) under the conditions described for pH_v measurement. Images were processed with Photoshop software.

Online supplemental material

Fig. S1 shows purification of IFNAR1 for analysis of ubiquitin chains, expression of ubiquitin mutants, and effect of the lysine-less mutant on IFNAR1 degradation. Fig. S2 shows that dextran colocalized with lysosomal markers. Fig. S3 shows the effect of pH on the binding of anti-IFNAR1 antibody to the receptor chain and effect of the lysine-less ubiquitin mutant on IFNAR1 sorting. Fig. S4 shows the effect of the expression of ubiquitin mutants on the clathrin-dependent internalization of IFNAR1. Table S1 presents a comparison of relative protein abundance in samples from cells expressing either IFNAR1^{WT} or vector. Online supplemental material is available at http://www.jcb.org/cgi/content/full/jcb.200706034/DC1.

We thank S. Royle, Y. Yarden, V. Haucke, Z.-Q. Pan, J. Wade Harper, and S. Pellegrini for the reagents. We are also grateful to A. Sorkin, J.A. Diehl, and V.S. Spiegelman for helpful comments and suggestions.

This work was supported by Public Health Service grants from the National Institutes of Health (CA092900 to S.Y. Fuchs and AG025688 to J. Peng), by a grant from the Canadian Cystic Fibrosis Foundation (to H. Barriere), and by grants from the Canadian Institutes of Health Research and National Institute of Diabetes and Digestive and Kidney Diseases (to G.L. Lukacs).

Submitted: 6 June 2007
Accepted: 6 November 2007

References

Barriere, H., C. Nemes, D. Lechardeur, M. Khan-Mohammad, K. Fruh, and G.L. Lukacs. 2006. Molecular basis of oligoubiquitin-dependent internalization of membrane proteins in mammalian cells. *Traffic*. 7:282–297.

Blondel, M.O., J. Morvan, S. Dupre, D. Urban-Grimal, R. Haguenauer-Tsapis, and C. Volland. 2004. Direct sorting of the yeast uracil permease to the endosomal system is controlled by uracil binding and Rsp5p-dependent ubiquitylation. *Mol. Biol. Cell*. 15:883–895.

Bonifacino, J.S., and L.M. Traub. 2003. Signals for sorting of transmembrane proteins to endosomes and lysosomes. *Annu. Rev. Biochem.* 72:395–447.

Bonifacino, J.S., and A.M. Weissman. 1998. Ubiquitin and the control of protein fate in the secretory and endocytic pathways. *Annu. Rev. Cell Dev. Biol.* 14:19–57.

Brzovic, P.S., and R.E. Klevit. 2006. Ubiquitin transfer from the E2 perspective: why is UbcH5 so promiscuous? *Cell Cycle*. 5:2867–2873.

Chastagner, P., A. Israel, and C. Brou. 2006. Itch/AIP4 mediates Deltex degradation through the formation of K29-linked polyubiquitin chains. *EMBO Rep.* 7:1147–1153.

Chuang, E., M.L. Alegre, C.S. Duckett, P.J. Noel, M.G. Vander Heiden, and C.B. Thompson. 1997. Interaction of CTLA-4 with the clathrin-associated protein AP50 results in ligand-independent endocytosis that limits cell surface expression. *J. Immunol.* 159:144–151.

Constantinescu, S.N., E. Croze, C. Wang, A. Murti, L. Basu, J.E. Mullersman, and L.M. Pfeffer. 1994. Role of interferon alpha/beta receptor chain 1 in the structure and transmembrane signaling of the interferon alpha/beta receptor complex. *Proc. Natl. Acad. Sci. USA*. 91:9602–9606.

Dikic, I. 2003. Mechanisms controlling EGF receptor endocytosis and degradation. *Biochem. Soc. Trans.* 31:1178–1181.

Duncan, L.M., S. Piper, R.B. Dodd, M.K. Saville, C.M. Sanderson, J.P. Luzio, and P.J. Lehner. 2006. Lysine-63-linked ubiquitination is required for endolysosomal degradation of class I molecules. *EMBO J.* 25:1635–1645.

Dupre, S., D. Urban-Grimal, and R. Haguenauer-Tsapis. 2004. Ubiquitin and endocytic internalization in yeast and animal cells. *Biochim. Biophys. Acta*. 1695:89–111.

Ea, C.K., L. Deng, Z.P. Xia, G. Pineda, and Z.J. Chen. 2006. Activation of IKK by TNFalpha requires site-specific ubiquitination of RIP1 and polyubiquitin binding by NEMO. *Mol. Cell*. 22:245–257.

French, M., K. Swanson, S.C. Shih, I. Radhakrishnan, and L. Hicke. 2005. Identification and characterization of modular domains that bind ubiquitin. *Methods Enzymol.* 399:135–157.

Fuchs, S.Y., A. Chen, Y. Xiong, Z.Q. Pan, and Z. Ronai. 1999. HOS, a human homolog of Slimb, forms an SCF complex with Skp1 and Cullin1 and targets the phosphorylation-dependent degradation of IkappaB and beta-catenin. *Oncogene*. 18:2039–2046.

Fuchs, S.Y., V.S. Spiegelman, and K.G. Kumar. 2004. The many faces of beta-TrCP E3 ubiquitin ligases: reflections in the magic mirror of cancer. *Oncogene*. 23:2028–2036.

Galan, J.M., and R. Haguenauer-Tsapis. 1997. Ubiquitin lys63 is involved in ubiquitination of a yeast plasma membrane protein. *EMBO J.* 16:5847–5854.

Geetha, T., J. Jiang, and M.W. Wooten. 2005. Lysine 63 polyubiquitination of the nerve growth factor receptor TrkA directs internalization and signaling. *Mol. Cell*. 20:301–312.

Goldman, L.A., M. Zafari, E.C. Cutrone, A. Dang, M. Brickelmeier, L. Runkel, C.D. Benjamin, L.E. Ling, and J.A. Langer. 1999. Characterization of antihuman IFNAR-1 monoclonal antibodies: epitope localization and functional analysis. *J. Interferon Cytokine Res.* 19:15–26.

Haglund, K., P.P. Di Fiore, and I. Dikic. 2003a. Distinct monoubiquitin signals in receptor endocytosis. *Trends Biochem. Sci.* 28:598–603.

Haglund, K., S. Sigismund, S. Polo, I. Szymkiewicz, P.P. Di Fiore, and I. Dikic. 2003b. Multiple monoubiquitination of RTKs is sufficient for their endocytosis and degradation. *Nat. Cell Biol.* 5:461–466.

Hammond, D.E., S. Carter, J. McCullough, S. Urbe, G. Vande Woude, and M.J. Clague. 2003. Endosomal dynamics of Met determine signaling output. *Mol. Biol. Cell*. 14:1346–1354.

Harper, J.W., J.L. Burton, and M.J. Solomon. 2002. The anaphase-promoting complex: it's not just for mitosis any more. *Genes Dev.* 16:2179–2206.

Hawryluk, M.J., P.A. Keyel, S.K. Mishra, S.C. Watkins, J.E. Heuser, and L.M. Traub. 2006. Epsin 1 is a polyubiquitin-selective clathrin-associated sorting protein. *Traffic*. 7:262–281.

Hicke, L., and R. Dunn. 2003. Regulation of membrane protein transport by ubiquitin and ubiquitin-binding proteins. *Annu. Rev. Cell Dev. Biol.* 19:141–172.

Hoeller, D., N. Crosetto, B. Blagoev, C. Raiborg, R. Tikkanen, S. Wagner, K. Kowanetz, R. Breitling, M. Mann, H. Stenmark, and I. Dikic. 2006. Regulation of ubiquitin-binding proteins by monoubiquitination. *Nat. Cell Biol.* 8:163–169.

Huang, F., D. Kirkpatrick, X. Jiang, S. Gygi, and A. Sorkin. 2006. Differential regulation of EGF receptor internalization and degradation by multiubiquitination within the kinase domain. *Mol. Cell*. 21:737–748.

Jin, J., T. Shirogane, L. Xu, G. Nalepa, J. Qin, S.J. Elledge, and J.W. Harper. 2003. SCFbeta-TRCP links Chk1 signaling to degradation of the Cdc25A protein phosphatase. *Genes Dev.* 17:3062–3074.

Kamsteeg, E.J., G. Hendriks, M. Boone, I.B. Konings, V. Oorschot, P. van der Sluijs, J. Klumperman, and P.M. Deen. 2006. Short-chain ubiquitination mediates the regulated endocytosis of the aquaporin-2 water channel. *Proc. Natl. Acad. Sci. USA*. 103:18344–18349.

Kanayama, A., R.B. Seth, L. Sun, C.K. Ea, M. Hong, A. Shaito, Y.H. Chiu, L. Deng, and Z.J. Chen. 2004. TAB2 and TAB3 activate the NF-kappaB pathway through binding to polyubiquitin chains. *Mol. Cell*. 15:535–548.

Kirkpatrick, D.S., N.A. Hathaway, J. Hanna, S. Elsasser, J. Rush, D. Finley, R.W. King, and S.P. Gygi. 2006. Quantitative analysis of in vitro ubiquitinated cyclin B1 reveals complex chain topology. *Nat. Cell Biol.* 8:700–710.

Kumar, K.G., W. Tang, A.K. Ravindranath, W.A. Clark, E. Croze, and S.Y. Fuchs. 2003. SCF(HOS) ubiquitin ligase mediates the ligand-induced down-regulation of the interferon-alpha receptor. *EMBO J.* 22:5480–5490.

Kumar, K.G., J.J. Krolewski, and S.Y. Fuchs. 2004. Phosphorylation and specific ubiquitin acceptor sites are required for ubiquitination and degradation of the IFNAR1 subunit of type I interferon receptor. *J. Biol. Chem.* 279:46614–46620.

Levkowitz, G., H. Waterman, E. Zamir, Z. Kam, S. Oved, W.Y. Langdon, L. Beguinot, B. Geiger, and Y. Yarden. 1998. c-Cbl/Sli-1 regulates endocytic sorting and ubiquitination of the epidermal growth factor receptor. *Genes Dev.* 12:3663–3674.

Li, M., C.L. Brooks, F. Wu-Baer, D. Chen, R. Baer, and W. Gu. 2003. Mono- versus polyubiquitination: differential control of p53 fate by Mdm2. *Science*. 302:1972–1975.

Li, Y., K.G. Kumar, W. Tang, V.S. Spiegelman, and S.Y. Fuchs. 2004. Negative regulation of prolactin receptor stability and signaling mediated by SCF(beta-TrCP) E3 ubiquitin ligase. *Mol. Cell. Biol.* 24:4038–4048.

Marijanovic, Z., J. Ragimbeau, K.G. Kumar, S.Y. Fuchs, and S. Pellegrini. 2006. TYK2 activity promotes ligand-induced IFNAR1 proteolysis. *Biochem. J.* 397:31–38.

Mosesson, Y., K. Shtiegman, M. Katz, Y. Zwang, G. Vereb, J. Szollosi, and Y. Yarden. 2003. Endocytosis of receptor tyrosine kinases is driven by monoubiquitylation, not polyubiquitylation. *J. Biol. Chem.* 278:21323–21326.

Mukherjee, S., R.N. Ghosh, and F.R. Maxfield. 1997. Endocytosis. *Physiol. Rev.* 77:759–803.

Muller, U., U. Steinhoff, L.F. Reis, S. Hemmi, J. Pavlovic, R.M. Zinkernagel, and M. Aguet. 1994. Functional role of type I and type II interferons in antiviral defense. *Science*. 264:1918–1921.

Ohmura-Hoshino, M., Y. Matsuki, M. Aoki, E. Goto, M. Mito, M. Uematsu, T. Kakiuchi, H. Hotta, and S. Ishido. 2006. Inhibition of MHC class II expression and immune responses by c-MIR. *J. Immunol.* 177:341–354.

Petroski, M.D., and R.J. Deshaies. 2005. Function and regulation of cullin-RING ubiquitin ligases. *Nat. Rev. Mol. Cell Biol.* 6:9–20.

Pickart, C.M., and D. Fushman. 2004. Polyubiquitin chains: polymeric protein signals. *Curr. Opin. Chem. Biol.* 8:610–616.

Polo, S., S. Confalonieri, A.E. Salcini, and P.P. Di Fiore. 2003. EH and UIM: endocytosis and more. *Sci. STKE*. doi:10.1126/stke.2132003re17.

Ragimbeau, J., E. Dondi, A. Alcover, P. Eid, G. Uze, and S. Pellegrini. 2003. The tyrosine kinase Tyk2 controls IFNAR1 cell surface expression. *EMBO J.* 22:537–547.

Raiborg, C., T.E. Rusten, and H. Stenmark. 2003. Protein sorting into multivesicular endosomes. *Curr. Opin. Cell Biol.* 15:446–455.

Rao, N., A.K. Ghosh, S. Ota, P. Zhou, A.L. Reddi, K. Hakezi, B.K. Druker, J. Wu, and H. Band. 2001. The non-receptor tyrosine kinase Syk is a target of Cbl-mediated ubiquitylation upon B-cell receptor stimulation. *EMBO J.* 20:7085–7095.

Rohde, G., D. Wenzel, and V. Haucke. 2002. A phosphatidylinositol (4,5)-bisphosphate binding site within mu2-adaptin regulates clathrin-mediated endocytosis. *J. Cell Biol.* 158:209–214.

Royle, S.J., N.A. Bright, and L. Lagnado. 2005. Clathrin is required for the function of the mitotic spindle. *Nature*. 434:1152–1157.

Seet, B.T., I. Dikic, M.M. Zhou, and T. Pawson. 2006. Reading protein modifications with interaction domains. *Nat. Rev. Mol. Cell Biol.* 7:473–483.

Sharma, M., F. Pampinella, C. Nemes, M. Benharouga, J. So, K. Du, K.G. Bache, B. Papsin, N. Zerangue, H. Stenmark, and G.L. Lukacs. 2004. Misfolding diverts CFTR from recycling to degradation: quality control at early endosomes. *J. Cell Biol.* 164:923–933.

Shcherbik, N., T. Zoladek, J.T. Nickels, and D.S. Haines. 2003. Rsp5p is required for ER bound Mga2p120 polyubiquitination and release of the processed/tethered transactivator Mga2p90. *Curr. Biol.* 13:1227–1233.

Shin, J.S., M. Ebersold, M. Pypaert, L. Delamarre, A. Hartley, and I. Mellman. 2006. Surface expression of MHC class II in dendritic cells is controlled by regulated ubiquitination. *Nature*. 444:115–118.

Shiratori, T., S. Miyatake, H. Ohno, C. Nakaseko, K. Isono, J.S. Bonifacino, and T. Saito. 1997. Tyrosine phosphorylation controls internalization of CTLA-4 by regulating its interaction with clathrin-associated adaptor complex AP-2. *Immunity*. 6:583–589.

Sigismund, S., S. Polo, and P.P. Di Fiore. 2004. Signaling through monoubiquitination. *Curr. Top. Microbiol. Immunol.* 286:149–185.

Sigismund, S., T. Woelk, C. Puri, E. Maspero, C. Tacchetti, P. Transidico, P.P. Di Fiore, and S. Polo. 2005. Clathrin-independent endocytosis of ubiquitinated cargos. *Proc. Natl. Acad. Sci. USA*. 102:2760–2765.

Smythe, E., and G. Warren. 1991. The mechanism of receptor-mediated endocytosis. *Eur. J. Biochem.* 202:689–699.

Stamenova, S.D., M.E. French, Y. He, S.A. Francis, Z.B. Kramer, and L. Hicke. 2007. Ubiquitin binds to and regulates a subset of SH3 domains. *Mol. Cell*. 25:273–284.

Tan, P., S.Y. Fuchs, A. Chen, K. Wu, C. Gomez, Z. Ronai, and Z.Q. Pan. 1999. Recruitment of a ROC1-CUL1 ubiquitin ligase by Skp1 and HOS to catalyze the ubiquitination of I kappa B alpha. *Mol. Cell*. 3:527–533.

Tang, W., O.A. Pavlish, V.S. Spiegelman, A.A. Parkhitko, and S.Y. Fuchs. 2003. Interaction of Epstein-Barr virus latent membrane protein 1 with SCFHOS/beta-TrCP E3 ubiquitin ligase regulates extent of NF-kappaB activation. *J. Biol. Chem.* 278:48942–48949.

Traub, L.M., and G.L. Lukacs. 2007. Decoding ubiquitin sorting signals for clathrin-dependent endocytosis by CLASPs. *J. Cell Sci.* 120:543–553.

van Kerkhof, P., R. Govers, C.M. Alves dos Santos, and G.J. Strous. 2000. Endocytosis and degradation of the growth hormone receptor are proteasome-dependent. *J. Biol. Chem.* 275:1575–1580.

van Niel, G., R. Wubbolts, T. Ten Broeke, S.I. Buschow, F.A. Ossendorp, C.J. Melief, G. Raposo, B.W. van Balkom, and W. Stoorvogel. 2006. Dendritic cells regulate exposure of MHC class II at their plasma membrane by oligoubiquitination. *Immunity*. 25:885–894.

Winston, J.T., P. Strack, P. Beer-Romero, C.Y. Chu, S.J. Elledge, and J.W. Harper. 1999. The SCFbeta-TRCP-ubiquitin ligase complex associates specifically with phosphorylated destruction motifs in IkappaBalpha and beta-catenin and stimulates IkappaBalpha ubiquitination in vitro. *Genes Dev.* 13:270–283.

Wu, G., G. Xu, B.A. Schulman, P.D. Jeffrey, J.W. Harper, and N.P. Pavletich. 2003. Structure of a beta-TrCP1-Skp1-beta-catenin complex: destruction motif binding and lysine specificity of the SCF(beta-TrCP1) ubiquitin ligase. *Mol. Cell*. 11:1445–1456.

Wu, K., A. Chen, P. Tan, and Z.Q. Pan. 2002. The Nedd8-conjugated ROC1-CUL1 core ubiquitin ligase utilizes Nedd8 charged surface residues for efficient polyubiquitin chain assembly catalyzed by Cdc34. *J. Biol. Chem.* 277:516–527.

Xu, P., and J. Peng. 2006. Dissecting the ubiquitin pathway by mass spectrometry. *Biochim. Biophys. Acta*. 1764:1940–1947.

Yan, H., K. Krishnan, A.C. Greenlund, S. Gupta, J.T. Lim, R.D. Schreiber, C.W. Schindler, and J.J. Krolewski. 1996. Phosphorylated interferon-alpha receptor 1 subunit (IFNaR1) acts as a docking site for the latent form of the 113 kDa STAT2 protein. *EMBO J.* 15:1064–1074.

Zhang, Y., and J.P. Allison. 1997. Interaction of CTLA-4 with AP50, a clathrin-coated pit adaptor protein. *Proc. Natl. Acad. Sci. USA*. 94:9273–9278.